INL/EXT-19-55551-Revision-0

Creep-Fatigue Behavior and Damage Accumulation of a Candidate Structural Material for Concentrating Solar Power Thermal Receiver Quarter 6 Report

Michael D McMurtrey, Ryann E Rupp,
Bipul Barua, Mark Messner

August 2019

Idaho National Laboratory

The INL is a U.S. Department of Energy National Laboratory
operated by Battelle Energy Alliance

INL/EXT-19-55551-Revision-0

Creep-Fatigue Behavior and Damage Accumulation of a Candidate Structural Material for Concentrating Solar Power Thermal Receiver Quarter 6 Report

Michael D McMurtrey, Ryann E Rupp, Bipul Barua, Mark Messner

August 2019

Idaho National Laboratory
Idaho Falls, Idaho 83415

http://www.inl.gov

Prepared for the
U.S. Department of Energy
Office of Energy Efficiency and Renewable Energy
Under DOE Idaho Operations Office
Contract DE-AC07-05ID14517

Research Performance Progress Report (RPPR) – DOE Solar Program

Project Title: Creep-fatigue Behavior and Damage Accumulation of a Candidate Structural Material for Concentrating Solar Power Solar Thermal Receiver

Project Period: 2/01/18 – 1/31/20

Budget Period: 5/01/19 – 7/31/19

Reporting Period: 5/01/19 – 7/31/119

Reporting Frequency: Quarterly

Submission Date: 8/15/19

Recipient: Idaho National Laboratory

Address: 2525 Fremont Ave
Idaho Falls, ID 83402

Website (if available) www.inl.gov

Project Number: 33872

Project Team: Idaho National Laboratory
Argonne National Laboratory

Principal Investigator: Michael McMurtrey, Materials Scientist
Phone: (208) 526-2327
Email: michael.mcmurtrey@inl.gov

Business Contact: Gabriel Ilevbare**,** Materials Science & Engineering Manager
Phone: 208-526-3735
Email: gabriel.ilevbare@inl.gov

HQ Tech Manager: Mark Lausten

HQ Project Officer: Christine Bing

GO Grant Specialist: GS name

GO Contracting Officer: CO name

8/15/19 .

Signature **Date**

Information from Statement of Project Objectives (SOPO)

Project Objective**:** Creep-fatigue deformation is an important consideration for a thermal receiver in Concentrating Solar Power (CSP) systems due to the constant static stress or pressure, diurnal cycling, and elevated service temperatures required for efficient operation. An accurate description of the creep-fatigue behavior, not available for five of the six candidate materials, is important for assessment of preliminary designs. This project will provide a detailed analysis of the creep-fatigue behavior and damage accumulation of a candidate structural material for a CSP solar thermal receiver to address a critical knowledge barrier for receiver designs identified in the CSP Gen3 Demonstration Roadmap. This effort includes the development of rules for the design of solar receiver components against high temperature creep-fatigue and ratcheting failure modes. The ASME Code rules for high temperature nuclear components will form the basis of the method but adjustments will be made to reflect the generally shorter, diurnal operating cycles of thermal receivers and the relative consequences of failure, comparing nuclear to solar components.

Work Planned for this Quarter**:**

Task 1 – All initial planned fatigue conditions were previously, however some additional fatigue and creep-fatigue data was generated this quarter to strengthen design curves.

Task 2 – Not much was changed in the design models, though some new data was added. Test/example cases were performed to demonstrate use of the model.

Task 3 – Force controlled testing was performed on Alloy 740H plate for comparison to the upcoming sheet testing that will need to be run in force control.

Plans for Next Quarter**:**

Task 1 – Creep-fatigue testing will be finalized with additional data to ensure confidence in the Task 2 design models..

Task 2 – Design rules and models will continue to be refined and finalized with data generated by INL.

Task 3 – Additional force controlled plate testing will be performed (at 750°C), as well as initial sheet specimen tests.

Narrative Report and Update:

Project Results and Discussion:

Task 1

No additional data was generated in creep or tensile testing this quarter. The completed datasets for tensile and creep testing are shown in the previous (Q5) report. New fatigue and creep-fatigue testing generated this quarter was limited by required maintenance affecting two frames, resulting in fewer than expected available test frames. This issue has been resolved and a significant effort is underway to complete tests during Q7. In this quarter, a new fatigue and creep fatigue test were completed, as well as three load control tests that are related to Task 3 and will be covered in more detail within that section.

Fatigue and Creep-Fatigue Testing

Cyclic testing (including both fatigue and creep-fatigue) was performed using three-zone furnaces. Each zone may be controlled independently to ensure minimal temperature gradients over the gage section. Extensometers are used to measure stain directly in the gage section (through use of ceramic posts that connect to the specimen over the gage section). A window has been cut in the furnace insulation to allow the extensometer posts to reach the sample. Tests for Task 1 are all strain controlled, with a strain rate of 0.001 /s.

Fatigue and creep-fatigue testing will be shown jointly in this report to better highlight the detrimental effects of creep in cyclic testing. The creep portion of creep-fatigue occurs during holds at peak tensile strain. A hold at the minimum compressive strain was examined previously and found to be less detrimental to the fatigue life. Tensile dwell times were chosen to ensure more conservative results for the design models. Two new tests were performed this quarter for this task, a fatigue test at 750°C and a delta strain of 0.6% and a creep-fatigue test at 850°C, with a 0.4% delta strain and a 10 minute hold time.

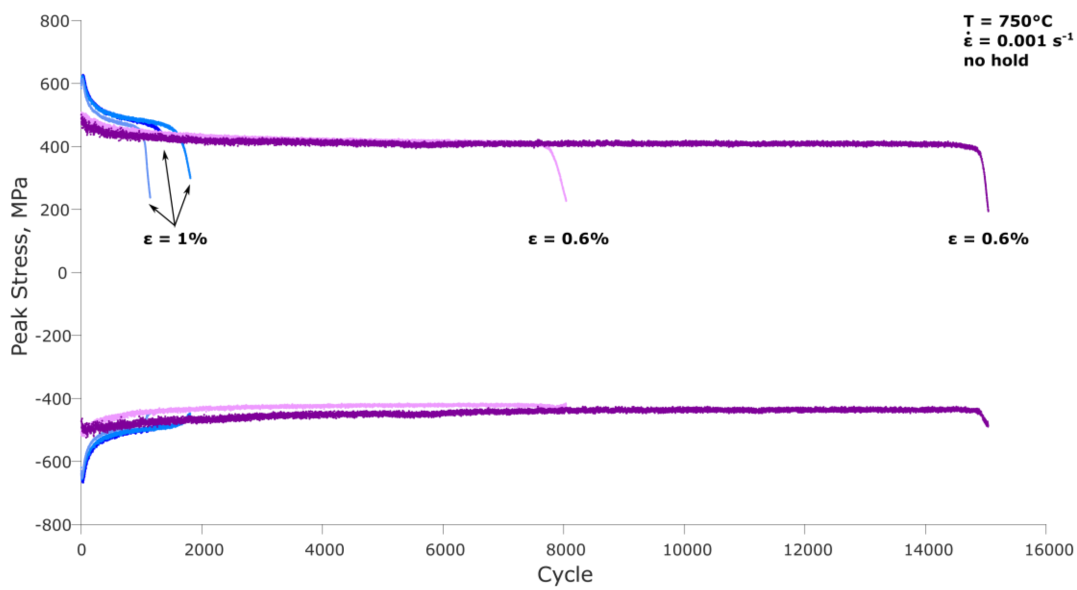

Figure 1. Fatigue curves for all strain controlled, 750°C tests.

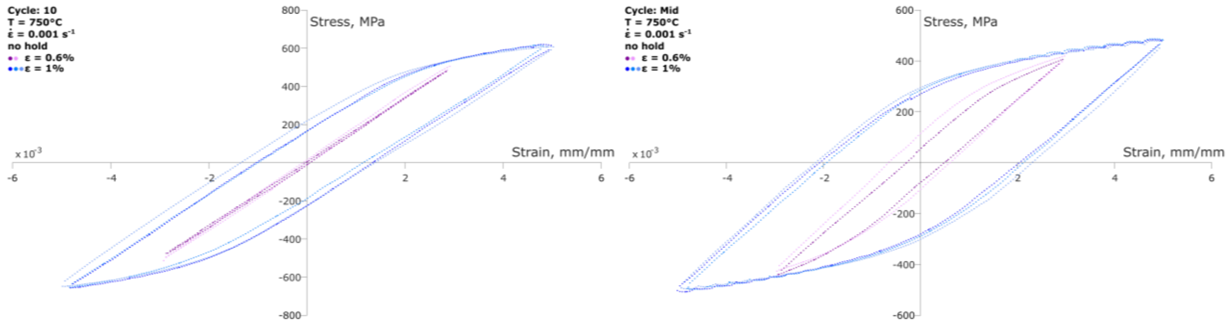

Figure 2. Hysteresis loops for cycle 10 (left) and the mid-cycle (right) for all strain controlled, 750°C fatigue tests.

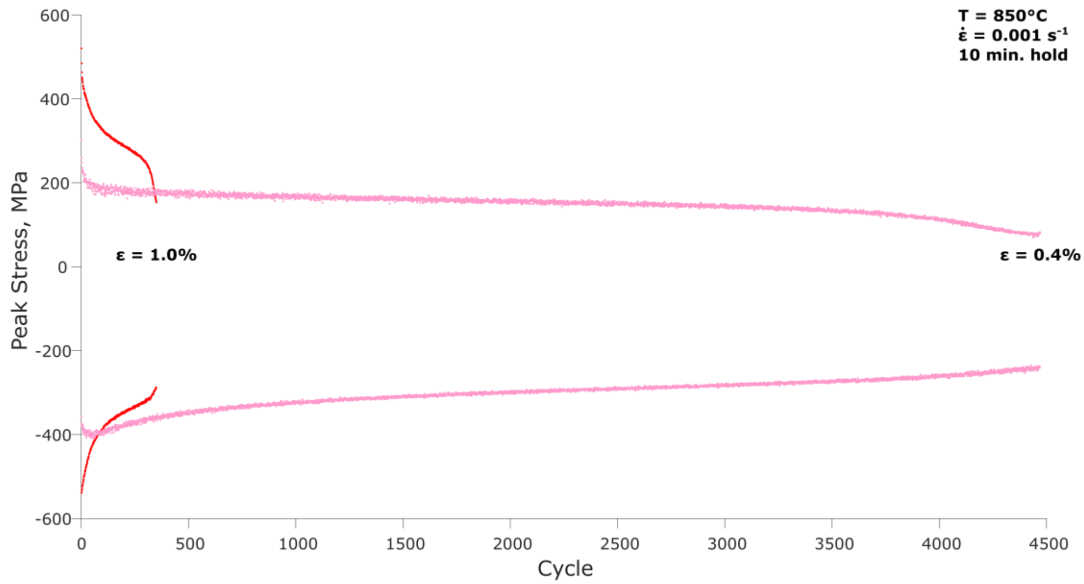

Figure 3. Creep-fatigue curves for both strain controlled, 850°C tests with a 10 minute hold in tension.

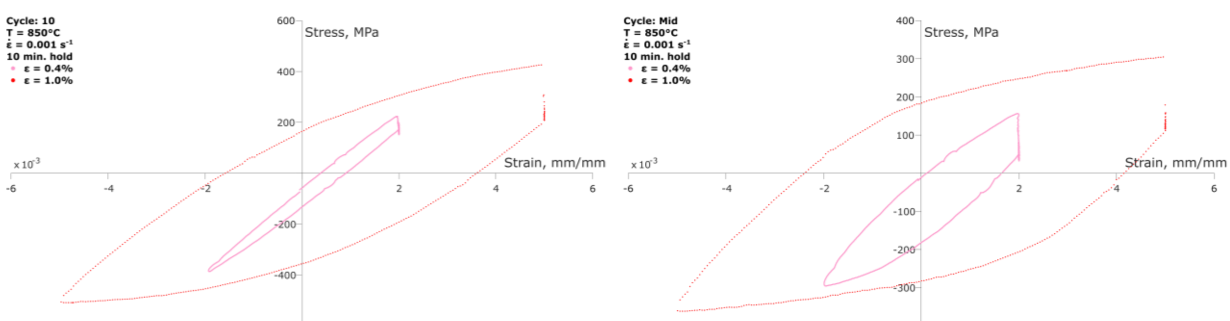

Figure 4. Hysteresis loops for cycle 10 (left) and mid-cycle (right) of both strain controlled, 850°C tests with a 10 minute hold in tension

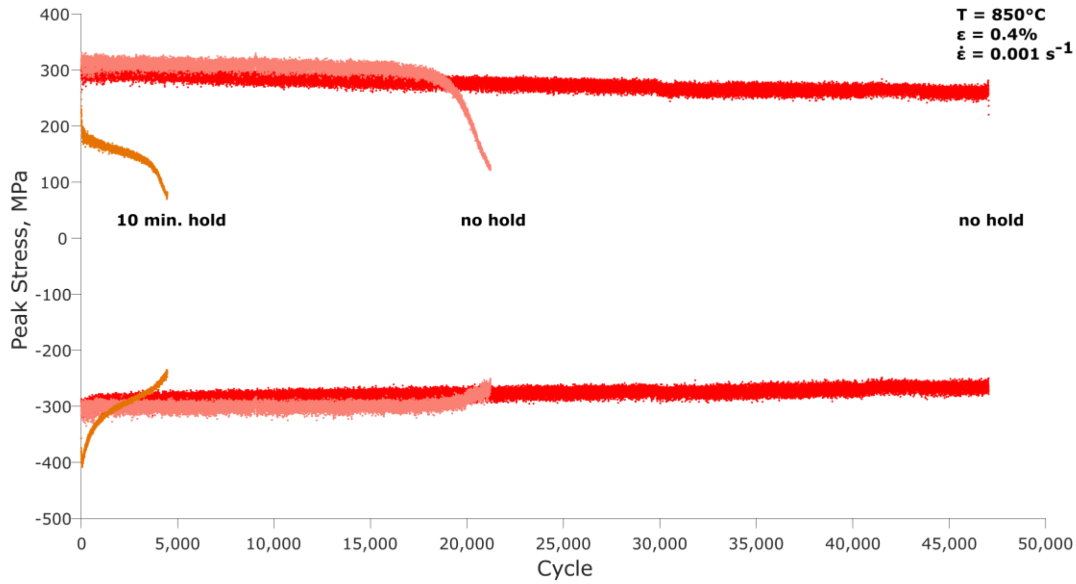

Figure 5. Stress vs. cycle for all strain controlled, 850°C with 0.4% total delta strain cyclic tests.

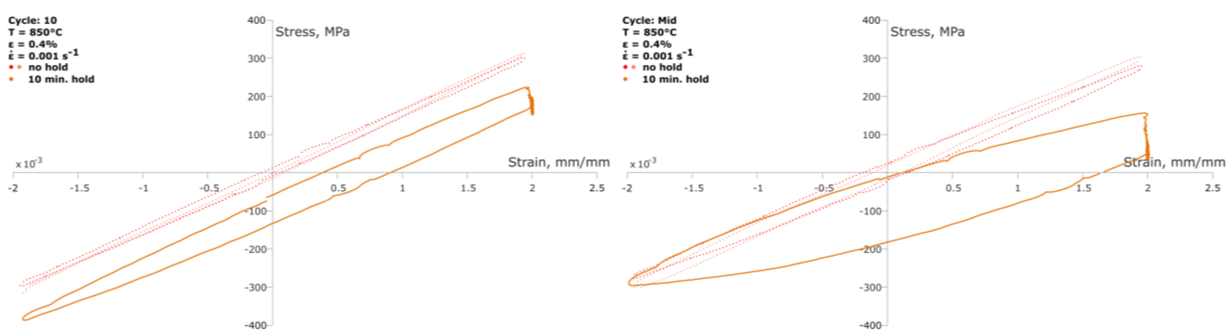

Figure 6. Hysteresis loops comparing 850°C fatigue and creep fatigue tests with a total delta strain of 0.4%. Cycle 10 is shown on the left and the mid-cycle to the right.

Summary

All of the fatigue and creep-fatigue testing is summarized in Table 1. The completed tests have been provided to ANL so that the design models may begin to be refined using actual test data. Significant testing, particularly creep-fatigue, will be performed in Q7 to ensure that the final design model has enough test data to provide confidence in the results. With additional test frames now available, no issues are expected with accomplishing the remaining tests.

Temp.	Strain Rate	Hold time[1]	$\Delta\varepsilon_t$	At Cycle 10				Midlife						
				σ_{max}	σ_{min}	$\sigma_{h\text{-}start}$	$\sigma_{h\text{-}end}$	cycle used	σ_{max}	σ_{min}	$\sigma_{h\text{-}start}$	$\sigma_{h\text{-}end}$	Cycles to Initiation	Cycles to Failure
(°C)	(/s)	(min)	(%)	(MPa)	(MPa)	(MPa)	(MPa)	$(N_{25}/2)$	(MPa)	(MPa)	(MPa)	(MPa)	(N_0)	(N_{25})
Fatigue testing														
750	0.001	0	0.6	508	-500	-	-	4000	420	-425	-	-	7827	7950
750	0.001	0	0.6	483	-479	-	-	7500	406	-440	-	-	14875	14987
750	0.001	0	1.0	610	-650	-	-	550	479	-496	-	-	1038	1095
750	0.001	0	1.0	620	-656	-	-	900	484	-508	-	-	-	-
750	0.001	0	1.0	616	-654	-	-	900	487	-498	-	-	1541	1767
800	0.001	0	1.0	554	-583			350	436	-450			637	653
850	0.001	0	0.4	313	-301	-	-	10000	305	-305	-	-	18619	19969
850	0.001	0	0.4	301	-297	-	-	20000	280	-277	-	-	-	47048[3,4]
850	0.001	0	1.0	516	-540	-	-	200	413	-428	-	-	398	409
850	0.001	0	1.0	514	-535	-	-	200	409	-417	-	-	370	402
Discarded Fatigue tests[2]														
850	0.001	0	1.0	423	-453	-	-	190	382	-403	-	-	353	377
750	0.001	0	1.0	579	-620	-	-	420	448	-475	-	-	821	848
750	0.001	0	1.0											747[3]
750	0.001	0	1.0											981[3]
750	0.001	0	1.0											693[3]
Creep-Fatigue testing														
750	0.001	60 T	1.0	578	-698	578	352	61	513	-676	513	274	111	122
750	0.001	60 C	1.0	665	-607	-607	-355	94	652	-527	-526	-275	181	187
750	0.001	600	1.0	Ongoing										
850	0.001	10 T	0.4	224	-386	224	173	2100	156	-296	155	48	3791	4147
850	0.001	10 T	1.0	426	-509	426	193	150	305	-362	305	104	320	342
850	0.001	10 T	1.0	456	-532	456	202	69	364	-422	363	132	-[4]	138[3,4]
850	0.001	600 T	1.0	311	-390	310	82	116	245	-299	244	51	209	231

Notes

1) In the case of hold times, T refers to a hold at peak tension stress and C refers to a hold at peak compressive stress

2) Testing using alternative methods of heating were found to vary the results and the data was not used in developing the design models

3) These cycles to failure are the total number of cycles performed by the test frame rather than the calculated 25% load drop from N_0)

4) Specimen cracked and failed outside the extensometer region

Table 1. Summary of Alloy 740H fatigue and creep-fatigue testing performed at INL. Tests that were not used in the design models are highlighted in red.

Task 2

Updated Alloy 740H design data

This section updates the design data for 740H based on the tests completed at INL in the current quarter. As mentioned in the previous quarterly report, the design information is essentially stable at this point. The only changes this quarter are to the fatigue diagram (negligible change) and to the creep-fatigue interaction diagram.

Young's modulus

No changes from our Q5 report. These values are from the material datasheet [1].

Temperature (°C)	Modulus (GPa)
20	221
100	218
200	212
300	206
400	200
500	193
600	186
700	178
800	169
900	160

Table 2. Design Young's modulus.

Poisson's ratio

Based on the ASME Section II Part D values we elect to use a constant value of 0.31. This is the same value recommended in our Q5 report.

Coefficient of thermal expansion

These values are from the material datasheet [1]. No change from our Q5 report.

Temperature (°C)	Mean CTE (µm/mm/°C)	Instantaneous CTE (µm/mm/°C)
20		12.38
100	12.38	12.38
200	13.04	13.55
300	13.5	14.32
400	13.93	15.12
500	14.27	15.55
600	14.57	16
700	15.03	17.68
800	15.72	20.39
900	16.41	16.51

Table 3. Design coefficients of thermal expansion.

Thermal conductivity

No change from our Q5 report. These values are from the material datasheet [1].

Temperature (°C)	Conductivity (W/(m °C))
20	10.2
100	11.7
200	13
300	14.5
400	15.7
500	17.1
600	18.4
700	20.2
800	22.1
900	23.8

Table 4. Design values of thermal conductivity.

Specific heat

No change from our Q5 report. These values are from the material datasheet [1].

Temperature (°C)	Specific heat (J/(kg °C))
20	449
100	476
200	489
300	496
400	503
500	513
600	519
700	542
800	573
900	635

Table 5. Design values of specific heat

Yield strength

No change from our Q5 report. These values are from the ASME Code Case [2].

Temperature (°C)	S_y (MPa)
40	621
100	594
150	577
200	562
250	548
300	538
350	531
400	529
450	529
500	529
550	529
600	529
650	529
700	529
750	508
800	463
850	418
900	373

Table 6. Design values of yield strength (S_y).

Ultimate tensile strength

No change from the Q5 report. These values are from the ASME Code Case [2].

Temperature (°C)	S_u (MPa)
40	1034
100	1034
150	1034
200	1030
250	998
300	976
350	967
400	966
450	966
500	966
550	966
600	957
650	921
700	860
750	771
800	651
850	531
900	411

Table 7. Design values of tensile strength (S_u).

Minimum rupture stress

No change from the Q5 report. These values were calculated from a rupture model developed at ANL using data from [3]. The line on the table indicates the region where the rupture stress is controlled by the material's ultimate tensile strength, instead of the creep rupture strength.

		Time (hours)									
		1	10	30	100	300	1000	3000	10000	30000	100000
Temp. (°C)	425	966	966	966	966	966	966	966	966	966	966
	450	966	966	966	966	966	966	966	966	966	966
	475	966	966	966	966	966	966	966	966	966	966
	500	966	966	966	966	966	966	966	966	966	966
	525	966	966	966	966	966	966	966	966	966	938
	550	966	966	966	966	966	966	966	966	876	749
	575	962	962	962	962	962	957	957	814	703	598
	600	957	957	957	957	957	902	775	656	563	476
	625	939	939	939	939	870	733	627	528	451	380
	650	921	921	921	834	710	595	507	424	361	302
	675	891	891	819	684	580	483	409	341	289	240
	700	860	800	675	561	473	392	331	274	231	191
	725	816	662	556	459	386	318	267	220	184	152
	750	771	548	458	376	314	258	215	176	147	120
	775	665	453	377	308	256	209	173	141	117	96
	800	555	374	310	252	208	169	140	113	94	76
	825	463	309	255	206	169	137	112	91	74	60
	850	386	255	209	168	138	111	90	73	59	48
	875	322	211	172	137	112	89	73	58	47	38
	900	268	174	141	112	91	72	58	46	38	30

Table 8: Design rupture stresses (S_r) in MPa.

Allowable stress S_o

No change from our Q5 report. These values are from the ASME Code Case [2].

Temperature (°C)	S_o (MPa)
40	295
100	295
150	295
200	279
250	276
300	276
350	276
400	276
450	276
500	276
550	276
600	274
650	226
700	146
750	84.1
800	34.5
850	21.8
900	13.8

Table 9. Allowable stress S_o.

Allowable stress S_m

Table 10 is provided for use with the Section III, Division 5, Nonmandatory Appendix T rules for ratcheting and creep-fatigue design by inelastic analysis. These values are the minimum of $0.9S_y$ and $S_u/3$ for the indicated temperatures.

Temperature (°C)	S_m (MPa)
40	345
100	345
150	345
200	343
250	333
300	325
350	322
400	322
450	322
500	322
550	322
600	319
650	307
700	287
750	257
800	217
850	177
900	137

Table 10. Allowable stress S_m.

Isochronous stress-strain curves

The model remains the same as in the Q5 report. The curves are based on an additive, history-independent decomposition of the total strain, ε into elastic strain, ε_e, time-independent plastic strain, ε_p, and time-dependent creep strain, ε_c.

$$\varepsilon = \varepsilon_e + \varepsilon_p + \varepsilon_c$$

The hot tensile curves are the outcome of this model when $\varepsilon_c = 0$, i.e. when $t = 0$, whereas the isochronous curves are the output of the model for some fixed, non-zero time. The elastic strain is calculated using the temperature dependent values of Young's modulus, E (Table 2) for Alloy 740H.

$$\varepsilon_e = \frac{\sigma}{E}$$

The plastic response of Alloy 740H was divided into two regions based on temperature. At temperatures below and equal to 800° C the composite model uses a Ramberg-Osgood model for the plastic strain to capture the experimentally-observed smooth transition from elastic to work hardening plastic behavior. Above this temperature the model uses a Voce hardening model to capture a quick transition to a nearly perfectly-plastic response. The composite model for the plastic strain is then

$$\varepsilon_p = \begin{cases} \begin{cases} 0 & \sigma \le \sigma_0 \\ K\left(\frac{\sigma-\sigma_0}{\sigma_0}\right)^n & \sigma > \sigma_0 \end{cases} & 600℃ \le T \le 800℃ \\ \begin{cases} 0 & \sigma \le \sigma_1 \\ \frac{-1}{\delta}\ln\left(1-\frac{\sigma-\sigma_1}{\sigma_p-\sigma_1}\right) & \sigma > \sigma_1 \end{cases} & T > 800℃ \end{cases}$$

Table 11 lists all the model constants for Ramberg-Osgood and Voce Hardening models for temperature range between 600℃ and 850℃.

Temperatures	Ramberg-Osgood model parameters			Voce hardening model parameters		
	σ_0(MPa)	K	n	σ_p(MPa)	σ_1(MPa)	δ
600°C - 700°C	400.24	0.0704	6.6480			
725°C	374.20	0.0357	7.1315			
750°C	348.16	0.0181	7.6150			
775°C	312.255	0.0055	10.971			
800°C	276.35	0.0017	14.327	574.991	455.850	908.324
825°C				521.631	319.315	2212.205
850°C				468.271	182.780	3516.087

Table 11. Parameters for plasticity models for ε_p.

To model the time-dependent strain, ε_c we adopt a simple creep model for alloy 740H.

$$\varepsilon_c = \dot{\varepsilon}_c(T,\sigma)t$$

where $\dot{\varepsilon}_c$ is some constant, average creep rate, which is a function of temperature and stress.

We adopt a form developed by Kocks [6] and Mecking [7] for the creep rate model. Their model posits a linear relation between the log-normalized material flow stress $\log\frac{\sigma}{\mu}$ and the normalized activation energy $\frac{kT}{\mu b^3}\ln\frac{\dot{\varepsilon}_0}{\dot{\varepsilon}}$. If this log-linear relation exists, the Kocks-Mecking model can be converted into a model for the deformation strain rate as a function of the linear fit slope A and intercept B

$$\dot{\varepsilon} = \dot{\varepsilon}_0 e^{B\mu b^3/(AkT)}\left(\frac{\sigma}{\mu}\right)^{-\mu b^3/(AkT)}$$

Here μ is the material shear stress given as $\mu = \frac{E}{2(1+\nu)}$, k is the Boltzmann constant, T is absolute temperature, b is a characteristic Burgers vector, and $\dot{\varepsilon}_0$ is some reference strain rate. Figure 7 plots the available Alloy 740H creep data using the average rate to 1% creep strain as the deformation strain rate and the applied values of stress and temperature.

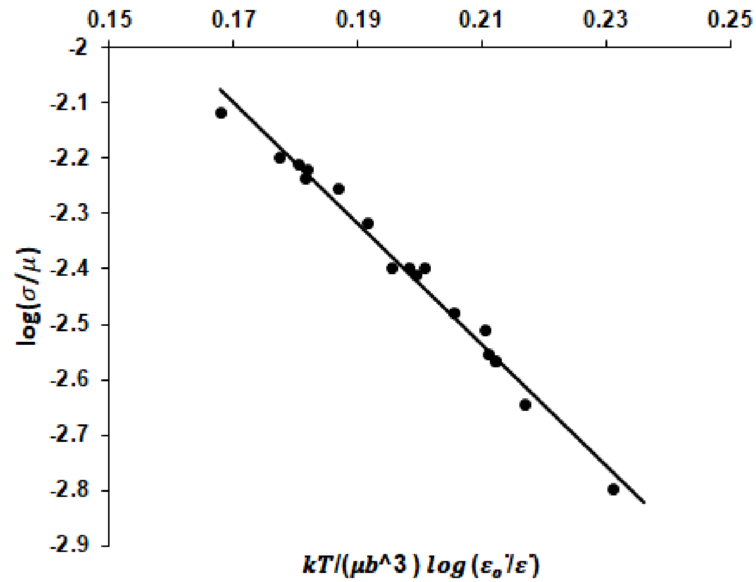

Figure 7. Kocks-Mecking diagram used to construct the model for ε_c.

As the Figure 7 shows, the Alloy 740 creep data nearly obeys the Kocks-Mecking form. Based on this diagram, the model for the creep strain adopted here is

$$\varepsilon_c = \dot{\varepsilon}_o e^{\frac{B\mu b^3}{AkT}} \left(\frac{\sigma}{\mu}\right)^{\frac{-\mu b^3}{AkT}} t$$

The parameters for the creep model are given in Table 12. Figures 8-18 plot the isochronous stress-strain curves for alloy 740H for temperatures in the range between 600°C and 850°C with an interval of 25°C.

$\dot{\varepsilon}_o$	1.19×10^{10} hr^{-1}
k	1.38064×10^{-20} mJ/K
b	2.53×10^{-07} mm
A	-10.98557
B	-0.53098

Table 12. Parameters for creep model of alloy 740H.

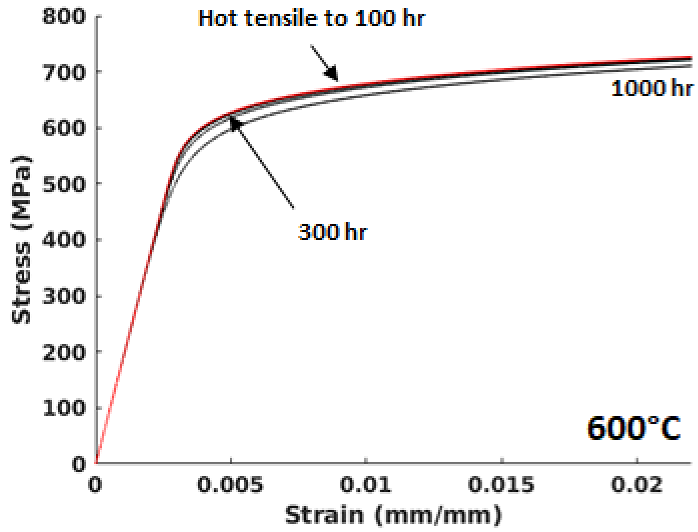

Figure 8. Isochronous stress strain curves at 600°C.

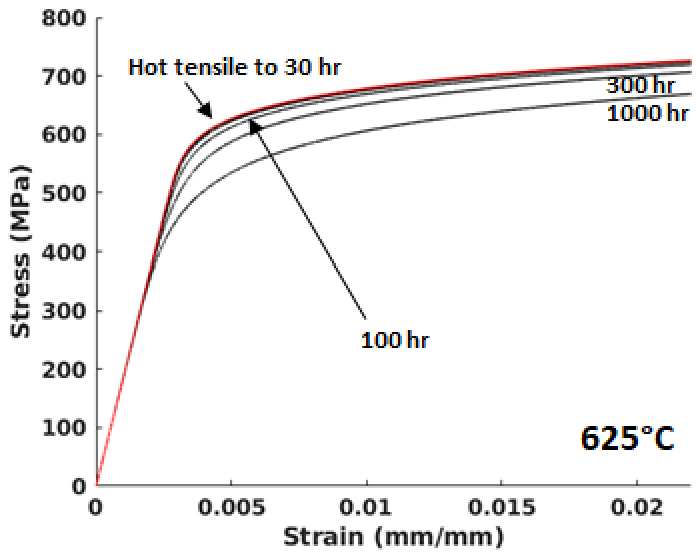

Figure 9. Isochronous stress strain curves at 625°C.

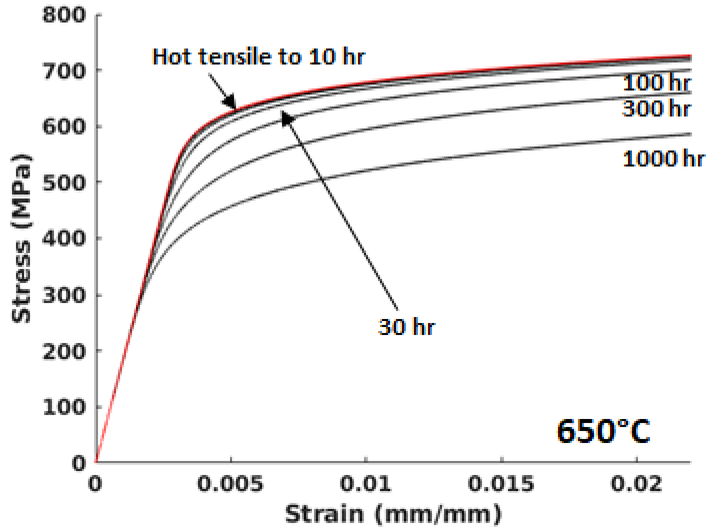

Figure 10. Isochronous stress strain curves at 650°C.

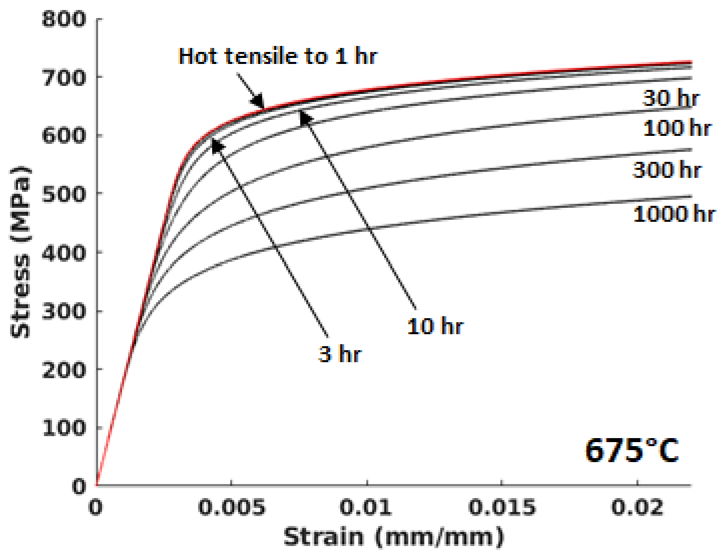

Figure 11. Isochronous stress strain curves at 675°C.

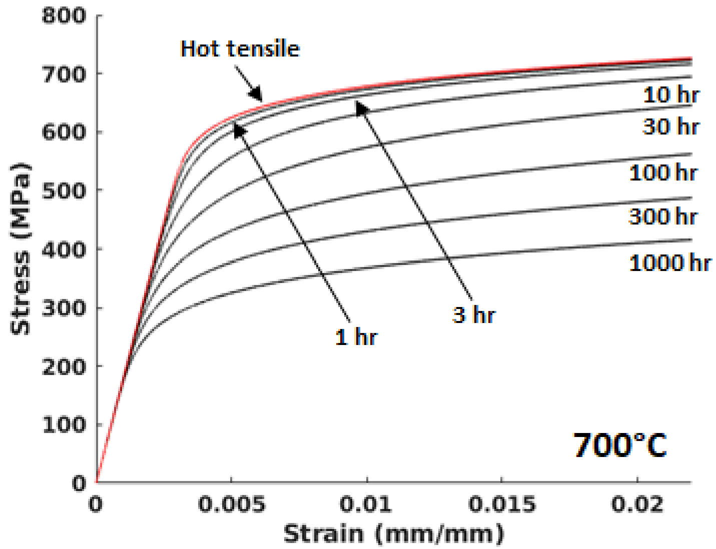

Figure 12. Isochronous stress strain curves at 700°C.

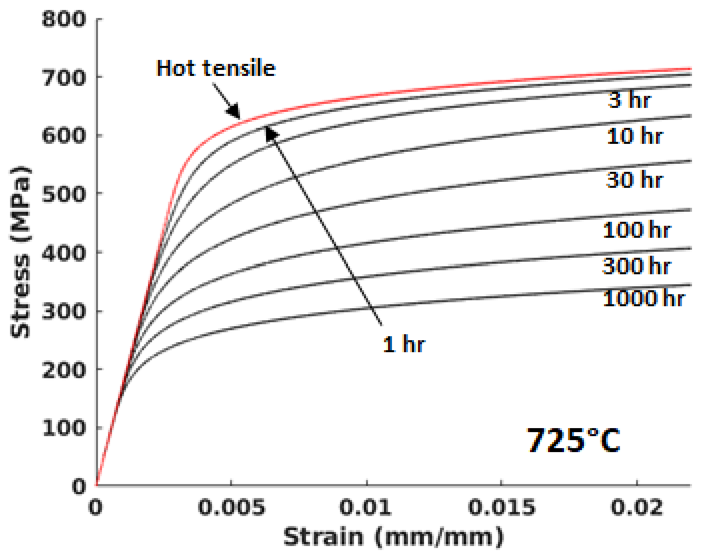

Figure 13. Isochronous stress strain curves at 725°C.

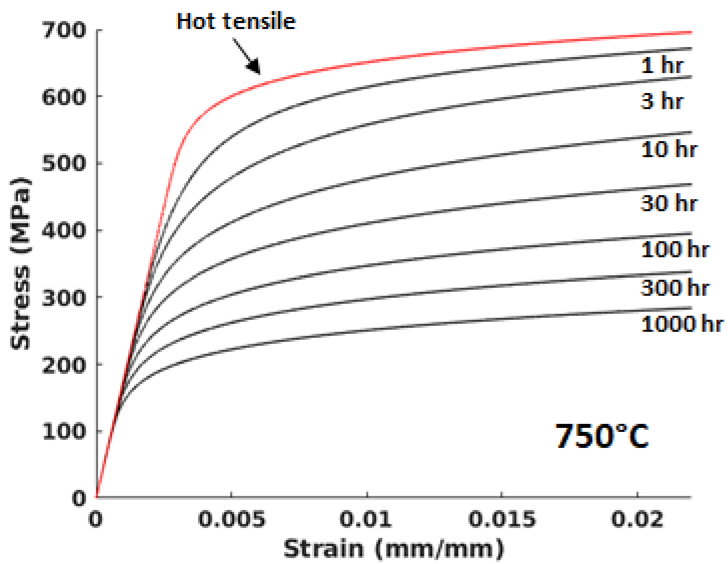

Figure 14. Isochronous stress strain curves at 750°C.

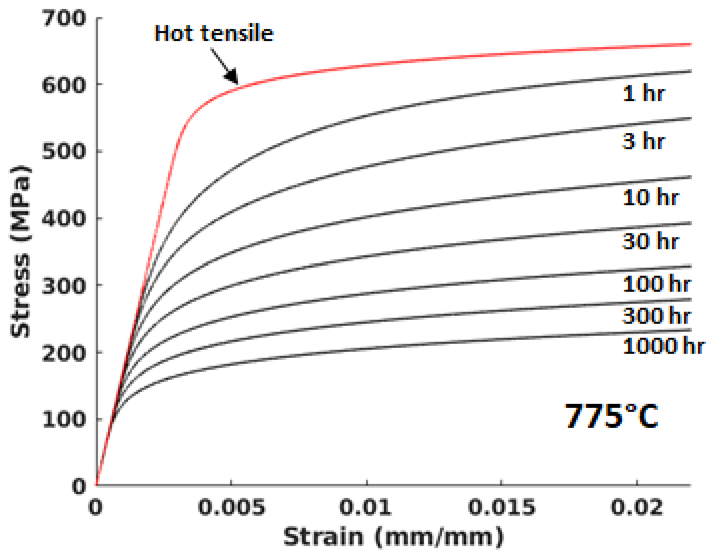

Figure 15. Isochronous stress strain curves at 775°C.

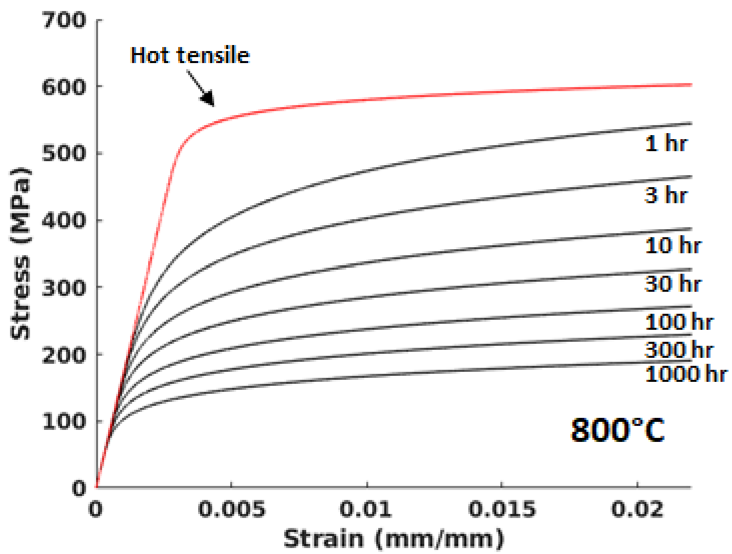

Figure 16. Isochronous stress strain curves at 800°C.

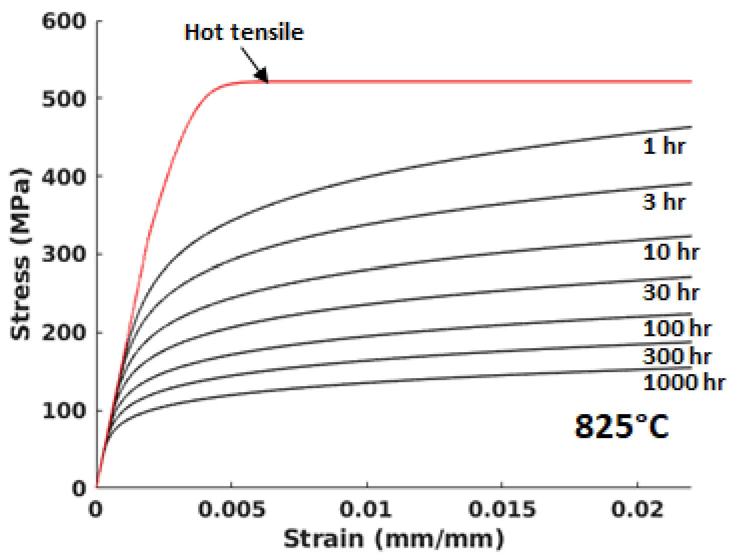

Figure 17. Isochronous stress strain curves at 825°C.

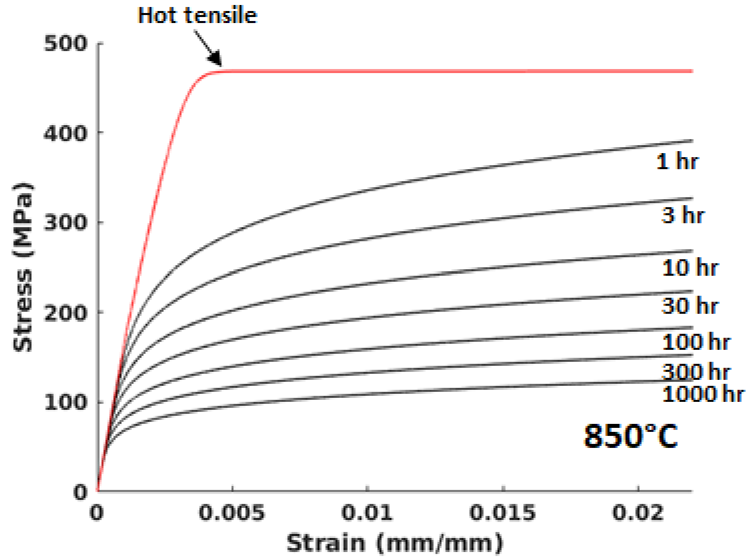

Figure 18. Isochronous stress strain curves at 850°C.

Relaxation strength

Section III, Division 5, Subsection HB, Subpart B, Nonmandatory Appendix T-1324 requires the use of a relaxation strength S_{rL} and S_{rH}. These values are not provided in the Code. For Alloy 740H designers may use the values tabulated in Table 13, which are based on stress relaxation using the creep model discussed above starting from a stress of $1.5S_m$.

		Time (hours)							
		1	10	30	100	300	1000	3000	10000
Temp. (°C)	425	483	483	483	483	483	483	483	483
	450	483	483	483	483	483	483	483	483
	475	483	483	483	483	483	483	483	483
	500	483	483	483	483	483	483	483	483
	525	483	483	483	483	483	483	483	483
	550	483	483	483	483	483	483	483	483
	575	481	481	481	481	481	481	481	481
	600	478	478	478	478	478	476	472	459
	625	469	469	469	468	466	460	445	412
	650	460	460	459	456	449	428	394	345
	675	445	444	441	432	412	374	328	278
	700	430	425	417	395	360	310	265	221
	725	406	395	377	340	296	248	208	172
	750	382	358	326	280	237	195	162	132
	775	348	308	270	224	186	151	124	101
	800	312	256	217	176	145	116	95	76
	825	272	207	171	137	111	88	71	57
	850	231	164	133	105	84	66	53	42

Table 13. Relaxation strength as a function of time and temperature. Values are in MPa.

Fatigue curves

One additional test from INL was included versus the Q5 report. This additional test did not significantly shift the design fatigue curves. The fatigue data comes from INL tests and the literature [4-5].

The fatigue curves are based on the correlations:

$$\Delta\varepsilon = \begin{cases} 0.0125N^{-0.08} + 0.0765N^{-0.44} & T \leq 700°\text{C} \\ 0.0393N^{-0.08} & 700°\text{C} < T \leq 850°\text{C} \end{cases}$$

to the available experimental data. The low temperature correlation was suggested by [5] and matches both the author's data and the new tests. The high temperature correlation is based on the INL test database. For both temperature ranges the recommended design fatigue curve are based on margins of 1.5 on strain range and 10 on cycles, i.e. if the nominal correlation is given by $\Delta\varepsilon(N)$ then the design correlation is based on $\Delta\varepsilon_{design}(N) = \min\{\Delta\varepsilon(N)/1.5, \Delta\varepsilon(N/10)\}$. Tables 14 and 15 list points along both the nominal and design fatigue curves.

Cycles	Strain range, nominal (mm/mm)	Strain range, design (mm/mm)
10	0.03817	0.025448
20	0.03031	0.020207
40	0.02440	0.016265
100	0.01873	0.012488
200	0.01562	0.010410
400	0.01322	0.008813
1000	0.01085	0.007236
2000	0.00950	0.006336
4000	0.00843	0.005618
10000	0.00731	0.004875
20000	0.00664	0.004427
40000	0.00608	0.004051
100000	0.00546	0.003639

Table 14. Fatigue curve for use below 700° C.

Cycles	Strain range, nominal (mm/mm)	Strain range, design (mm/mm)
10	0.02368154	0.01578769
20	0.0205589	0.01370593
40	0.01784801	0.01189867
100	0.01480505	0.00987004
200	0.01285286	0.00856857
400	0.01115809	0.00743872
1000	0.00925571	0.00617048
2000	0.00803526	0.00535684
4000	0.00697573	0.00465049
10000	0.00578642	0.00385761
20000	0.00502342	0.00334895
40000	0.00436104	0.00290736
100000	0.00361751	0.00241167

Table 15. Fatigue curve for use between 700° C and 850° C.

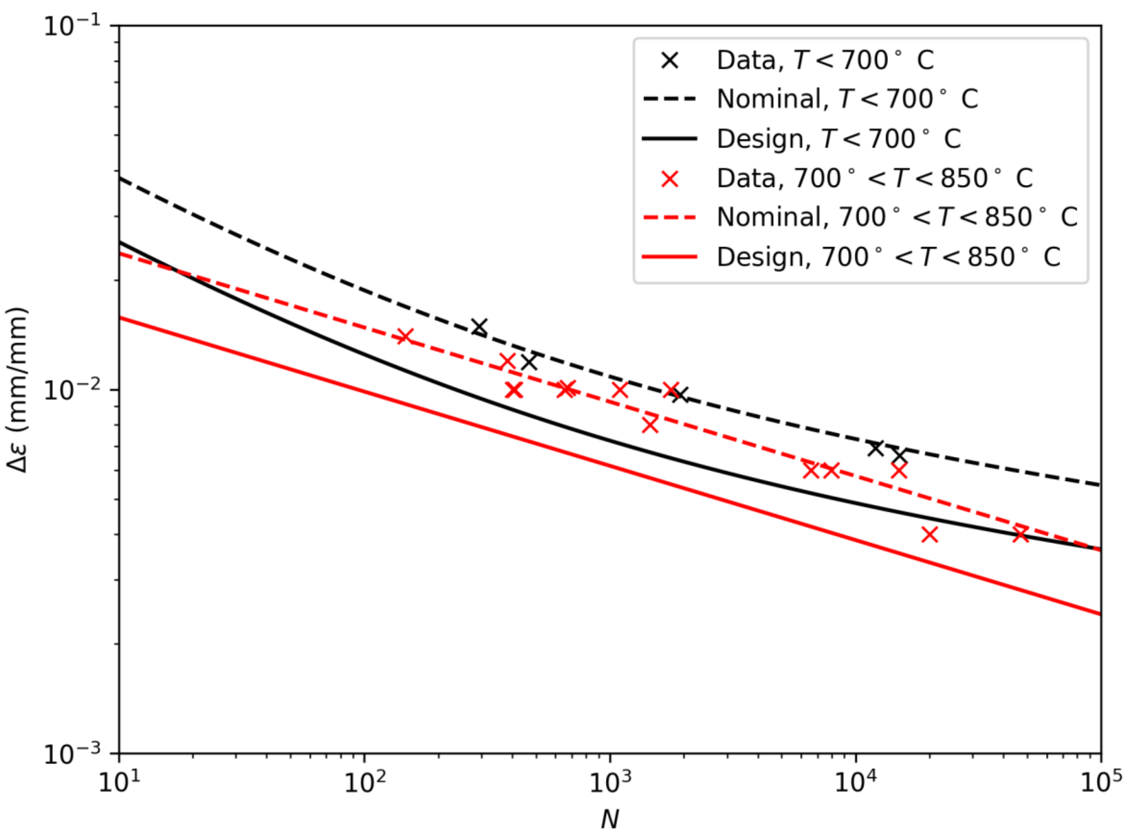

Figure 19. Nominal and design fatigue curves overlaid with fatigue data.

Creep-fatigue interaction diagram

The interaction diagram is based on creep-fatigue tests from INL and an additional data point gathered from the literature [8]. The literature datapoint is the outlier, falling underneath even the (0.1,0.1) intersection point plotted on the figure, drawn from the ASME A617 Code Case. This diagram was updated from Q5 with an additional test completed at INL. This additional test supports a more severe creep-fatigue interaction diagram, in line with the single datapoint collected from the literature. The final creep-fatigue interaction diagram will be determined once all the INL testing is complete.

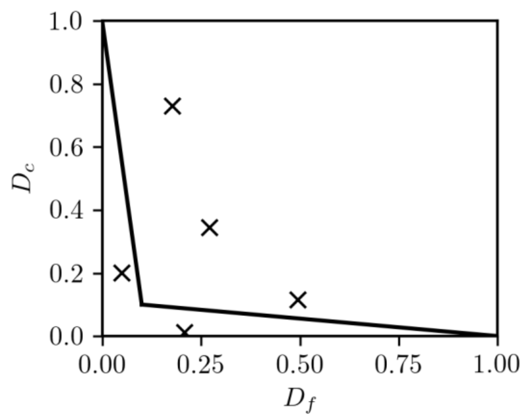

Figure 20. Creep fatigue-interaction diagram overlaid with experimental data
.

Sample problems illustrating the high temperature receiver design methods

The previous quarterly report identified three design methods suitable for the design of high temperature CSP components using Alloy 740H.

Method 1 is the classical ASME Section III, Division 5 design by elastic analysis method with a reduced design margin, making it suitable for use in CSP systems. This method is the most general in terms of materials and component types but the most difficult to execute.

Method 2 simplifies the ASME Section III, Division 5 method based on the high yield strength of Alloy 740H. Method 2 will produce comparable results to Method 1, but with much simpler design calculations.

Method 3 uses a simple inelastic analysis to analyze axisymmetric receiver structures. This method is relatively simple to execute but will produce the most accurate design calculations of high temperature life and therefore produce the most efficient designs. However, the method is limited to Alloy 740H and to certain types of load cycles, representative of CSP receivers but not of a broader class of components.

The below reproduces the description of each method provided in the Q5 report to aid the reader in following the sample problem calculations.

Method 1: ASME Section III, Division 5

The most general methods proposed here to use for design is the high temperature evaluation procedure described in Section III, Division 5, Subsection HB, Subpart B of the ASME Boiler and Pressure Vessel Code. This methodology was created to design safety-critical high temperature nuclear reactor components and so the provisions contain a large design margin to ensure safe performance. This design margin has been reduced somewhat for the Alloy 740H design data described above, to reflect the reduced safety requirements of CSP systems.

The specific design method proposed for use for CSP receivers is a simplification of the full Section III, Division 5 rules. In all cases the design data for 740H given above should be used in the analysis.

1. Define a series of service loads in terms of time-dependent mechanical and thermal boundary conditions on the structure. Each service case should define periodic loading conditions as well as provide an expected number of repetitions of this particular cycle type in service. Additionally, define a design loading based on enveloping the worst combinations of temperatures, pressures, and mechanical forces from the aggregate of all the service loading conditions, as described in HBB-3113.
2. Perform a transient elastic thermo-mechanical analysis of the component for each service load case. Follow the stress classification guidelines in Section III, Division 5, HBB-3213 to divide the loads in primary, local primary, secondary, and peak categories. Perform the same process for the design loading.
3. Check the primary stress from the design load analysis against the allowable stress S_o given above, as described in HBB-3222.1. The intent of this check is to replicate non-nuclear allowable stress design in Section VIII or Section I and so these Sections may be alternately used as a basis for primary load design, replacing this step.
4. Check the structure against the ratcheting criteria described in HBB-1332 (the O'Donnell-Porowski approach), with the following changes:
    a. The strain limit is increased to 2% for base metal and 1% for weld metal.
    b. The applicable temperature limit from Table HBB-T-1323 for 740H is $600°C$. We anticipate that the receiver temperatures will fall below this threshold during the night periods and so the method should be universally applicable.
    c. The strain calculation may be based on a stress of $1.0\sigma_c$ rather than the $1.25\sigma_c$ specified in the Code. The strain value need not exceed 2% divided by the total number of cycles.
5. Evaluate the structure against the creep-fatigue criteria described in HBB-1430 with the following modifications:
    a. When calculating the creep strain increment in HBB-1432 the stress intensity used is $1.0\sigma_c$ rather than the $1.25\sigma_c$ specified in the Code.
    b. When using HBB-1433 option (b) to determine a stress relaxation profile, the lower bound stress S_{LB} may be taken as $1.0\sigma_c$, rather than the $1.25\sigma_c$ specified in the Code.

6. The buckling exemption charts described in HBB-T-1520 deal with load-controlled buckling which is not applicable to CSP receivers, as the load-controlled compressive stresses are expected to be minimal. Furthermore, time-dependent strain-controlled buckling is generally not a significant concern and so for CSP receivers only strain-controlled time independent buckling is relevant. Buckling may be checked by analyzing the structure assuming a constitutive response given by the hot tensile curves described above and a load factor of 1.5. This is a slight reduction from the HBB factor of 1.67, reflecting the lower consequences of failure for CSP systems.

Method 2: Simplified elastic design for high strength materials

This method is a simplification of the ASME Section III, Division 5 method described above for Alloy 740H. One characteristic of this material is its high yield point, even at elevated temperatures. This means that the response of a receiver is likely to be well represented by an elastic-creep constitutive model, which simplifies the creep-fatigue evaluation using the Division 5 approach. Furthermore, hold times in the creep regime are short for CSP systems because of the diurnal cycling pattern and so it is conservative to assume no stress relaxation occurs during the loading. Steps 1, 2, 3, 4, and 6 remain the same as with Method 1. Step 5 is replaced with the following procedure.

This method is applicable only if the primary plus secondary stress intensity (P+Q) remains less than S_y for all service loading cycles and if the peak stresses are minimal.

For each service load cycle:

1. Calculate the transient stress versus time profile via elastic analysis.
2. Convert these stresses into elastic strains using the Young's modulus and Poisson's ratio provided above.
3. Compute creep damage
    a. Calculate an effective strain range $\Delta\varepsilon_1$ using HBB-T-1413.
    b. Calculate a strain due to creep, $\Delta\varepsilon_2$ by using the isochronous curves to calculate the creep-ratcheting strain accumulated through a single cycle period at a stress of σ_c, where σ_c is the O'Donnell-Porowski core stress determined in Method 1, Step 4.
    c. Determine the total strain range for this cycle as $\Delta\varepsilon = \Delta\varepsilon_1 + \Delta\varepsilon_2$.
4. Determine the stress versus time profile used to calculate creep damage for this cycle by calculating the von Mises stress from the elastically-calculated stresses derived in step 1. This effective stress versus time profile may be used in determining the creep damage attributed to this load cycle.

This process produces, at each material point, an effective strain range and a stress relaxation history. These individual cycle effective strains can be converted into a total fatigue damage using a rainflow counting approach and the definition of fatigue damage given in HBB-T-1411 (Miner's rule). The individual stress relaxation profiles can be combined using the procedure given in HBB-T-1433. Creep damage can be calculated from this composite history using the definition given in HBB-T-1411 and the resulting creep and fatigue damages assessed against the creep-fatigue interaction diagram.

If the loading cycles correspond to full daily receiver cycles so that the total number of service loading cycles, N, equals the plant operating life in days then the creep strain increment in step 3b may be estimated as $\Delta\varepsilon_2 = 0.02/N$, which will be negligible for many receiver designs.

Method 3: Simplified inelastic design for high strength materials

This approach is again limited to situations where the elastically-calculated stresses remain below the material yield stress S_y for all service cycles. Furthermore, this approach is limited to design situations where the service cycles correspond to full daily receiver loadings. Some small number of representative loadings may be used, however each of these representative cycles must correspond to a full daily loading. This provision means separate weather-related loads cannot be separated from a standard daily cycle – if any such loadings exist they must be incorporated into daily load cycles.

With these conditions met, an elastic-creep constitutive response reasonably describes the material. For small creep strains, this response can be characterized with the simple model determined above for use in constructing the material isochronous curves. This model is defined by:

$$\dot{\boldsymbol{\sigma}} = \boldsymbol{C}:\left(\dot{\boldsymbol{\varepsilon}} - \dot{\boldsymbol{\varepsilon}}_{cr} - \dot{\boldsymbol{\varepsilon}}_{th}\right)$$

where $\dot{\boldsymbol{\sigma}}$ is the stress rate, $\boldsymbol{C}$ is the isotropic elasticity tensor, defined through the elastic constants above, $\dot{\boldsymbol{\varepsilon}}$ is the total strain rate, $\dot{\boldsymbol{\varepsilon}}_{th}$ is the thermal strain rate, defined through the thermal expansion coefficients above, and $\dot{\boldsymbol{\varepsilon}}_{cr}$ is defined as

$$\dot{\boldsymbol{\varepsilon}}_{cr} = \dot{\varepsilon}\left(\sigma_{eff}\right)\frac{\boldsymbol{s}}{\|\boldsymbol{s}\|}$$

where $\boldsymbol{s}$ is the deviatoric stress, σ_{eff} is the von Mises effective stress, and $\dot{\varepsilon}(\sigma)$ is the scalar creep strain rate equation defined above as:

$$\dot{\varepsilon} = \dot{\varepsilon}_0 e^{B\mu b^3/(AkT)}\left(\frac{\sigma}{\mu}\right)^{-\mu b^3/(AkT)}.$$

These expressions extend the scalar model developed above to 3D using standard J_2 flow theory.

This design method follows Method 1 steps 1 to 3 for assessing primary load design. Additionally, the designer must check these elastically-calculated stresses to ensure the total primary + secondary (P+Q) stress intensity does not exceed S_y at any point during the service history. Buckling is assessed using step 6 from Method 1. However, ratcheting and creep-fatigue are assessed using the following modified procedure. This process must be applied at each material point in order to assess the suitability of the entire component.

For each load cycle:

1. Perform an elastic-creep analysis of the structure using the model defined above. Repeat this analysis for as many cycles as are required to achieve a steady cyclic response, defined by the stresses becoming periodic with the applied loads (see notes below).

2. Extract the stress/strain/time history for a single cycle of the periodic loading after the structure achieves a steady-state response.
    a. Calculate the effective strain range $\Delta\varepsilon$ using the definition given in HBB-T-1413.
    b. Extract the stress relaxation profile $\sigma_{eff}(t)$ given by plotting the von Mises effective stress versus time over this load cycle.
    c. Extract the effective ratcheting rate for this load cycle, Δr, by subtracting calculating the effective strain $\sqrt{\frac{2}{3}\boldsymbol{\varepsilon}:\boldsymbol{\varepsilon}}$ at the beginning (r_1) and end (r_2) of the cycle. Calculate the effective ratcheting rate as $\Delta r = |r_2 - r_1|$.

This process produces a histogram giving an effective strain range, effective stress history, and effective ratcheting rate for each cycle, along with the cycle frequency. The effective strain ranges are combined into a total fatigue damage using rainflow counting and Miner's rule. The effective stress histories are combined using the approach described in HBB-T-1411 and creep damage calculated from this history using HBB-T-1411, dividing the effective stress by a factor of 0.9 rather than the 0.67 specified in HBB-T-1411-1 of the ASME Code. The creep-fatigue diagram can then be consulted as an acceptance criteria.

The total ratcheting strain can be determined by

$$\varepsilon_r = \sum_{i=1}^{n_{type}} \Delta r_i N_i$$

where Δr_i is the effective ratcheting strain of cycle type i, N_i is the number of repetitions of this cycle type, and the sum proceeds over each service cycle. This sum must be less than 10% for base metal and 5% for welds at each material point. Note the ratcheting check is an integral part of this procedure because the creep model determined above is only valid up to a few percent strain.

The number of cycles required to achieve the cyclic steady state can be determined by plotting the effective von Mises stress as a function of time, shifted by the cycle period so that all the simulated cycles overlap. When the cycle stresses fall on top of one another sufficient cycles have been completed to achieve the cyclic steady-state solution.

Sample Problems

The remainder of this chapter then walks through two sample design problems, applying all three design methods to each problem. For the first sample problem the details provided in this report should be sufficient to provide a complete tutorial for designers describing how to execute the required design analysis and calculations.

Sample problem 1

Figure 21 illustrates the first problem considered for evaluating design methods developed for CSP systems. This problem is an axisymmetric representation of a tube in a cavity receiver. The tube is 500 mm long and 2 mm thick. The outer diameter is 40 mm. For simplicity, we assumed uniform the heat flux on the outer surface of the tube and that the heat conduction analysis is done in the steady state. This results in linear temperature gradient along the length, circumference, and thickness of the tube and therefore this problem can be treated as an axisymmetric problem. This linear temperature distribution can be fully described by providing the inner and outer tube metal temperatures as a function of time and axial position. Only two points are required to define the axial gradient. Figure 21 shows the temperature and pressure loading considered for this problem. The loading cycle includes warming up of the system in the morning, steady state operation, five cloud events each with 8 minutes hold, cooling down in the evening, and no operation during night. The design life of the tube is 30 years.

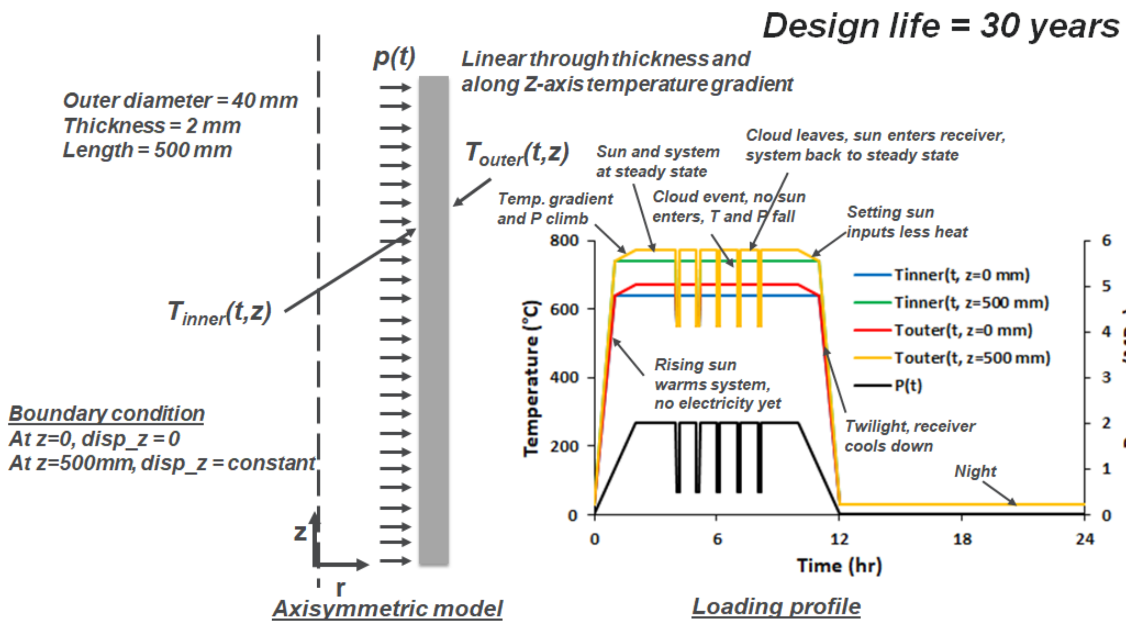

Figure 21: Sample problem 1. An axisymmetric representation of a single tube. Loading profile shows the inner and outer wall temperature at the bottom (z = 0 mm) and top (z = 500 mm) ends of the tube, respectively, and pressure exerted on the inner wall by the salt flowing inside the tube.

Design calculations based on Method 1

Step 1: Defining service loads and design loads

As we considered only one type of loading condition, the loading profile shown in Figure 21 can be considered as the design load. The daily load cycle can be divided into two service load types – start-up/shut-down cycle and cloud event. Table 16 provides the details of each service loads.

Service load types	Associated load points and time	Frequency per design cycle
start-up/shut-down cycle	Load point-1: 12 hours Load point-2: 12 hours	1
cloud event	Load point-2: 0 hours Load point-3: 0.133 hours	5

Table 16: Service load cycles and associated load points (illustrated in Figure 22) in the daily load cycle and corresponding hold times.

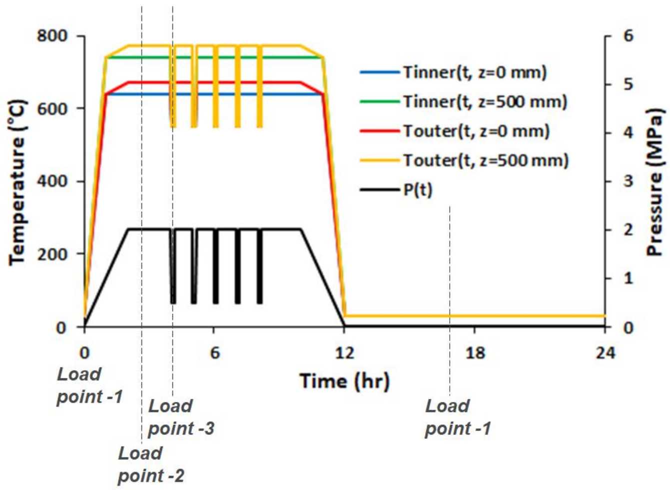

Figure 22: Different load points during the loading cycle considered.

Step 2: Transient elastic thermo-mechanical analysis for each service load case and stress classification

We used MOOSE (Multiphysics Object Oriented Simulation Environment), an open source finite element solver to perform the elastic thermo-mechanical analyses. We classify stresses due to pressure as primary load and thermal stresses caused by the temperature gradient as secondary load. There is no peak load.

Step 3: Primary load design check

Maximum primary load occurs at load point-2. Figure 23 shows the temperature distribution in the tube and stress components along the thickness of the tube at maximum wall averaged temperature location. Table 17 reports details of the primary load checks. First, all the stress components were linearized to divide into membrane and bending components along the stress classification line. The membrane and bending stress tensors were then used to determine the stress intensities in Table 17.

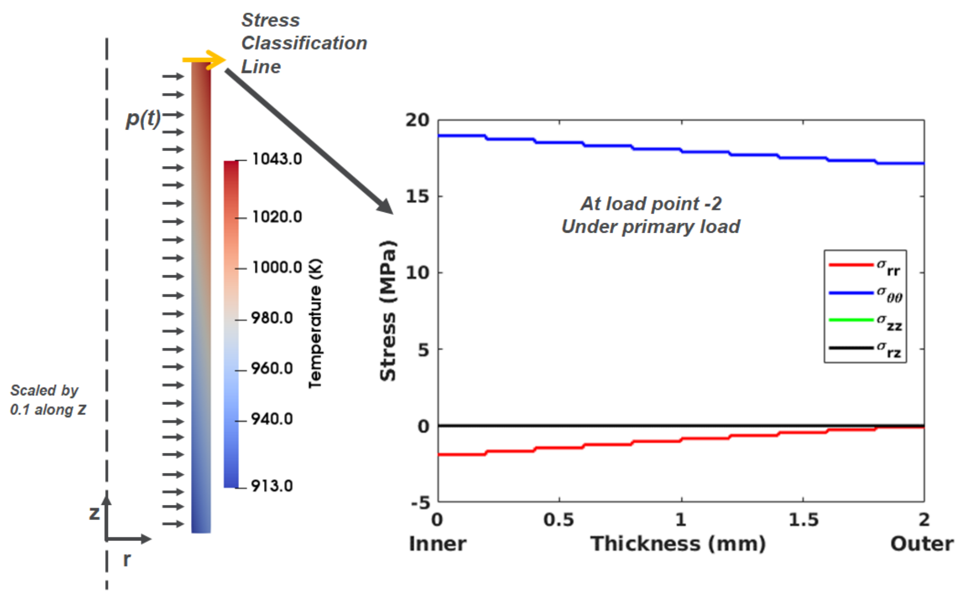

Figure 23: Temperature distribution in the tube and through thickness elastic stress components at maximum wall averaged temperature location under primary load at load point -2.

Max. General primary membrane stress intensity, P_m	18.95 MPa
Max. Combined primary membrane plus bending stress intensity, $P_L + P_b$	20.92 MPa
Maximum metal temperature, T_{max}	770 °C
Allowable stress, S_o at T_{max}	64.26 MPa
Design criteria -1: $P_m \leq S_o$	***PASS !***
Design criteria -2: $P_L + P_b \leq 1.5\, S_o$	***PASS !***

Table 17: Primary load design checks.

Step 4: Ratcheting check

Design Method 1 uses the O'Donnell-Porowski approach, described in Section III, Division 5, HBB-1332 for ratcheting checks. In this approach, an effective creep stress parameter, Z is determined from a primary stress parameter, X and a secondary stress parameter, Y as shown in Figure 24. The effective creep stress parameter is used to calculate the effective creep stress which is then used to determine the ratcheting creep strain using isochronous stress-strain curves. The definition of X and Y are

$X = (P_L + \frac{P_b}{K_t})_{max}/S_y$

$Y = (Q_R)_{max}/S_y$

where,

$(P_L + \frac{P_b}{K_t})_{max}/S_y$ = the maximum value of the primary stress intensity, adjusted for bending via K_t, during the cycle being evaluated.

$(Q_R)_{max}$ = the maximum range of the secondary stress intensity during the cycle being considered

S_y = is the average of the S_y values at the maximum and minimum wall averaged temperatures during the cycle

$K_t = (K + 1)/2$

K is 1.5 for across-the-wall bending of shell structures or rectangular sections, see HBB-3223 (c) (6) in Section III Division 5.

Once Z is found, effective core, σ_c stress is determined from

$Z = \frac{\sigma_c}{S_{yL}}$

where $S_{yL} = S_y$ at the cold end of the cycle being considered.

It should be noted that, the average wall temperature at one of the stress extremes defining the secondary stress intensity range must be below the temperature listed in Section III, Division 5, HBB-T-1323, given as 600°C for 740H in the description of the design method above.

The creep ratcheting strain increment for a load cycle is evaluated by entering the isochronous stress strain curves at the maximum wall temperature and effective core, σ_c stress during the load cycle with the stress held constant for the entire service life. An example of creep ratcheting strain determination is shown in Figure 25.

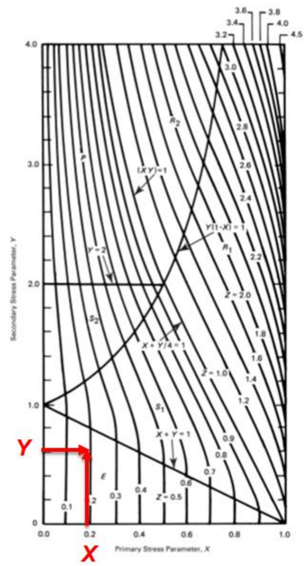

Figure 24: Determination of effective creep stress parameters from Section III, Division 5, Figure HBB-T-1332-1.

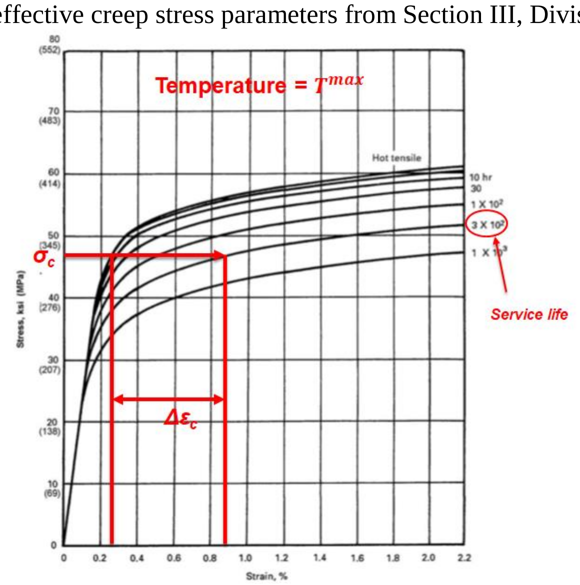

Figure 25: Determination of creep ratcheting strain increment from isochronous stress strain curves.

Since the start-up/shut-down service load includes the extreme temperature profile and the total time of the day, considering only the start-up/shut-down load should provide conservative estimation for ratcheting design. Table 18 provides all the calculation details of the ratcheting design check. Figure 26 shows the stress components under secondary loading at load point -2. Stress components are shown at two different locations – maximum wall averaged temperature and maximum von Mises stress. The maximum ratcheting strain in the structure is 5.82e-9% which is less than 2%, thus the design passes the ratcheting check. Note that, a design must pass the ratcheting design check before it is checked for creep-fatigue damage.

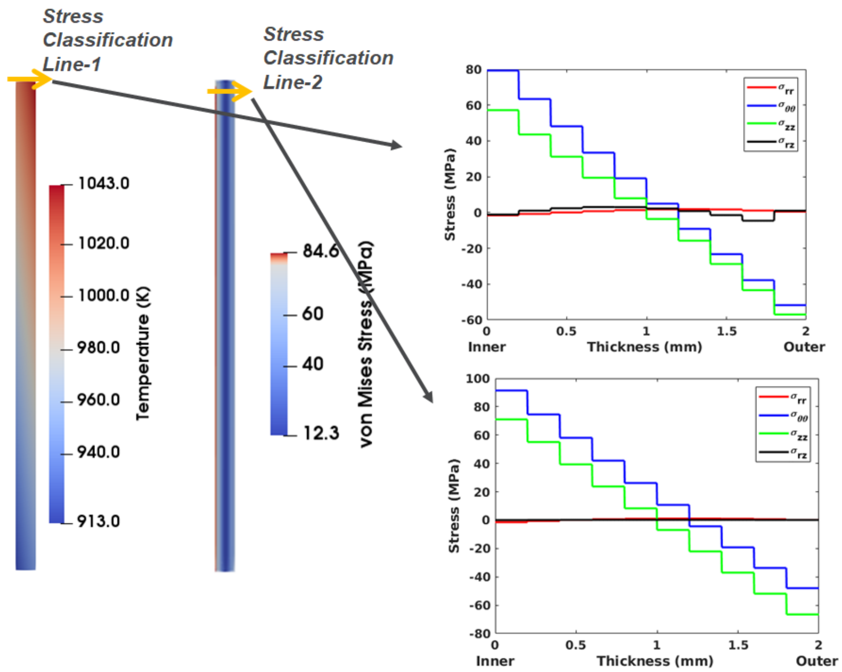

Figure 26: Temperature and von Mises stress distribution in the tube and through thickness stress components at maximum wall averaged temperature and maximum von Mises stress locations under secondary load at load point-2.

	Stress classification line-1 shown in Figure 26	***Stress classification line-2 shown in Figure 26***
$T^{max}_{wall\ averaged}$	755.2 °C	752.6 °C
$T^{min}_{wall\ averaged}$	30 °C	30 °C
T^{max}	770 °C	767.3 °C
S_{yH} (at $T^{max}_{wall\ averaged}$)	503.3 MPa	505.4 MPa
S_{yL} (at $T^{min}_{wall\ averaged}$)	621.0 MPa	621.0 MPa
$S_y = (S_{yH} + S_{yL})/2$	562.2 MPa	563.2 MPa
K	1.5	1.5
$K_t = (K+1)/2$	1.25	1.25
$(P_L + \frac{P_b}{K_t})_{max}$	20.53	20.53
$(Q_R)_{max}$	85.06	96.81
$X = (P_L + \frac{P_b}{K_t})_{max}/S_y$	0.037	0.036
$Y = (Q_R)_{max}/S_y$	0.151	0.172
Z using Section III, Division 5, Figure HBB-T-1332-1	0.037	0.036
σ_c from $Z = \frac{\sigma_c}{S_{yL}}$	22.67	22.63
Service life (considering whole day as service time per day)	30 years = 262800 hours	30 years = 262800 hours
Ratcheting strain at the end of service life	2.45e-8 %	6.41e-9 %
Ratcheting design criteria: 2% for base metal	***PASS!***	***PASS!***

Table 18: Ratcheting design check according to Method 1.

Step 5: Creep-fatigue damage check

According to Section III, Division 5, a design is acceptable if the creep and fatigue damage satisfy the following relation:

$$\sum_j \left(\frac{n}{N_d}\right)_j + \sum_k \left(\frac{\Delta t}{T_d}\right)_k \leq D$$

where D is the total creep-fatigue damage and the first and second terms on the left side are fatigue damage, D_f and creep damage, D_c, respectively. In the fatigue damage term, $(n)_j$ is the number of repetitions of cycle type j and $(N_d)_j$ is the number of design allowable cycles for respective cycle type; while in the creep damage term, $(T_d)_k$ is the allowable time duration for a given stress at the maximum temperature occurring in the time interval k and $(\Delta t)_k$ is the duration of the time interval k.

The design allowable cycles for fatigue damage is determined by entering fatigue curves at total strain range, ϵ_t. Total strain range, ϵ_t is calculated using equation HBB-T-1432-16:

$$\epsilon_t = K_v \Delta\epsilon_{mod} + K\Delta\epsilon_c$$

where K is the local geometric concentration or equivalent stress concentration factor determined by dividing effective primary plus secondary plus peak stress divided by the effective primary plus secondary stress, K_v is the multiaxial plasticity and Poisson ratio adjustment factor, $\Delta\epsilon_c$ is the creep strain increment, and $\Delta\epsilon_{mod}$ is the modified maximum equivalent strain range.

$\Delta\epsilon_{mod}$ is calculated using equation Section III, Division 5, HBB-T-1432-12:

$$\Delta\epsilon_{mod} = \left(\frac{S^*}{\bar{S}}\right) K^2 \Delta\epsilon_{max}$$

where $\Delta\epsilon_{max}$ is the maximum equivalent strain range calculated from the elastic analysis of under primary and secondary loading together. $\Delta\epsilon_{max}$ is calculated according to Section III, Division 5, HBB-T-1413 with $\nu^* = 0.3$ for elastic analysis. S^* and $\bar{S}$ are stresses determined by entering the isochronous stress-strain curves at $\Delta\epsilon_{max}$ and $K\Delta\epsilon_{max}$, respectively.

K_v is determined using equation Section III, Division 5, HBB-T-1432-15:

$$K_v = 1.0 + f(K_v' - 1.0)$$

where f is the inelastic multiaxial adjustment factor determined using Section III, Division 5, Figure HBB-T-1432-2 and triaxiality factor, T.F.

$$T.F. = \frac{|\sigma_1 + \sigma_2 + \sigma_3|}{\frac{1}{\sqrt{2}}[(\sigma_1 - \sigma_2)^2 + (\sigma_2 - \sigma_3)^2 + (\sigma_3 - \sigma_1)^2]}$$

where σ's are principals stresses at the extreme of the stress cycle.

K_v' is the adjustment for inelastic biaxial Poisson's ratio determined from Section III, Division 5, Figure HBB-T-1432-3 using K_e.

$$K_e = \begin{cases} 1 & ; \quad K\Delta\epsilon_{max} \leq 3\bar{S}_m/E \\ \frac{K\Delta\epsilon_{max}E}{3\bar{S}_m} & ; \quad K\Delta\epsilon_{max} > 3\bar{S}_m/E \end{cases}$$

where

$$3\bar{S}_m = \begin{cases} 1.5\, S_m + S_{rH}; & \text{when only one of the extreme of the stress difference occurs at a temperature above those covered by Division 1, Subsection NB rules} \\ S_{rH} + S_{rL}; & \text{when both of the extreme of the stress difference occur at a temperature above those covered by Division 1, Subsection NB rules} \end{cases}$$

Here S_{rH} and S_{rL} are relaxation strengths associated with the temperatures at the hot and cold extremes of the stress cycle. These values are provided above in the 740H design data. The hot temperature condition is defined as the maximum operating temperature of the stress cycle. The hot time is equal to the portion of service life when wall averaged temperatures exceed 425°C. The cold temperature is defined as the colder of the two temperatures corresponding to the two stress extremes in the stress cycle. The cold time is again equal to the portion of service life when wall averaged temperatures exceed 425°C.

The creep strain increment per stress cycle, $\Delta\epsilon_c$ is determined by entering the isochronous stress-strain curves at σ_c and maximum metal temperature for the stress cycle time, including hold times between transient (instead of total service life). Alternatively, the creep accumulated during the entire service life divided by the number of stress cycles during the entire service life can also be used for calculating creep strain increment per stress cycle, $\Delta\epsilon_c$. We used the latter option.

The design allowable cycles, N_d is then calculated from design fatigue curve at maximum metal temperature and using total strain range, ϵ_t, as illustrated in Figure 27. Fatigue damage fraction, D_f is then determined from the ratio between design cycles and design allowable cycles for each cycle type and then adding them together.

Figure 28 shows the equivalent strain from elastic analysis between load points 1&2 and between load points 2&3 along two stress classification lines. Table 19 shows the details of all the relevant calculations to determine fatigue damage fraction.

Creep damage evaluation is done in accordance to HBB-T1433(b) but with one exception. The lower bound stress S_{LB} is taken as $1.0\sigma_c$, rather than the $1.25\sigma_c$ specified in the Code. First, stress relaxation profile is determined by entering the isochronous stress-strain curves at a strain level equal to ϵ_t and at hold-time temperature and determining the corresponding stress levels at varying times. However, this stress relaxation process should not be permitted to a stress level less than S_{LB}. This stress relaxation procedure results in a stress-time history similar to that illustrated in Figure 29. Using the stress-time history and hold-time temperature during the cycle creep damage fraction can be calculated according to the illustration in Figure 30. For creep damage fraction calculation, we only considered the start-up/shut-down service load cycle and the day time (12 hr) during the cycle. The time duration of the cloud events is already included in the start-up/shut-down service load cycle. Creep damage is not expected during night time (12 hr) of the start-up/shut-down service load cycle. Table 20 and 21 show the details of determining creep damage fraction, D_c from stress relaxation profile.

To determine whether the design passes the creep-fatigue damage check, the fatigue damage fraction, D_f and creep damage fraction, D_c are plotted on creep-fatigue interaction diagram as shown in Figure 30. If the (D_f, D_c) point falls inside the creep-fatigue damage envelop the design passes. As seen in Figure 31, the (D_f, D_c) points fall inside the creep-fatigue damage envelop which means the design passes for creep-fatigue damage check.

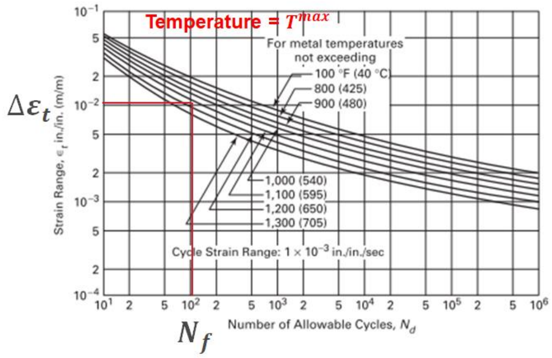

Figure 27: Illustration of determining design allowable cycles, N_d.

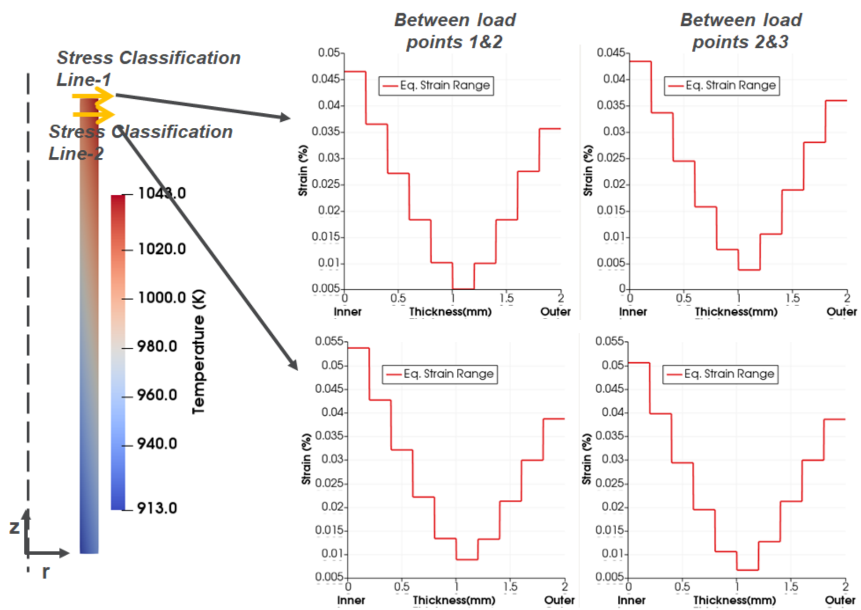

Figure 28: Equivalent strain range from elastic analysis.

	At OD on stress classification line-1 shown in Figure 28		***At OD on Stress classification line-2 shown in Figure 28***	
	Start-up/shut-down cycle	***Cloud event***	***Start-up/shut-down cycle***	***Cloud event***
T^{max}	770°C	770°C	767.3°C	767.3°C
Hot temperature	770°C	770°C	767.3°C	767.3°C
Cold temperature	30°C	550°C	30°C	550°C
Hot time	12hr*(30*365) =131400 hr	0	12hr*(30*365) =131400 hr	0
Cold time	12hr*(30*365) =131400 hr	8min*(30*365) =1460 hr	12hr*(30*365) =131400 hr	8min*(30*365) =1460 hr
S_{rH}	107.2 MPa	354.8 MPa	110.5 MPa	358.9 MPa
S_{rL}	Not required	153.3 MPa	Not required	158.4 MPa
S_m at T^{max}	241.0	Not required	243.2	Not required
$3\bar{S}_m$	468.7 MPa	508.1 MPa	475.3 MPa	517.3 MPa
$\Delta\epsilon_{max}$	0.0356 %	0.0360 %	0.0377 %	0.0376 %
K	1 (no peak stress)	1 (no peak stress)	1 (no peak stress)	1 (no peak stress)
$K\Delta\epsilon_{max}$	0.0356 %	0.0360 %	0.0377 %	0.0376 %
E	171700 MPa	171700 MPa	171943 MPa	171943 MPa
$3\bar{S}_m/E$	0.278 %	0.296 %	0.276 %	0.301 %
K_e	1	1	1	1
K'_v	1	1	1	1
K_v	1	1	1	1
$\frac{S^*}{S}$	1	1	1	1
$\Delta\epsilon_{mod}$	0.0356 %	0.0360 %	0.0377 %	0.0376 %
$\Delta\epsilon_c$	2.23e-12%	0	6.05e-13%	0
ϵ_t	0.0356 %	0.0360 %	0.0377 %	0.0376 %
Design allowable cycles, N_d	> 1e12	> 1e12	> 1e12	> 1e12
Design cycles, n	30*365=10950	30*365*5=54750	30*365=10950	30*365*5=54750
Fatigue damage fraction, D_f	***6.57e-8***		***6.57e-8***	

Table 19: Sample calculation of fatigue damage fraction, D_f according to Method 1.

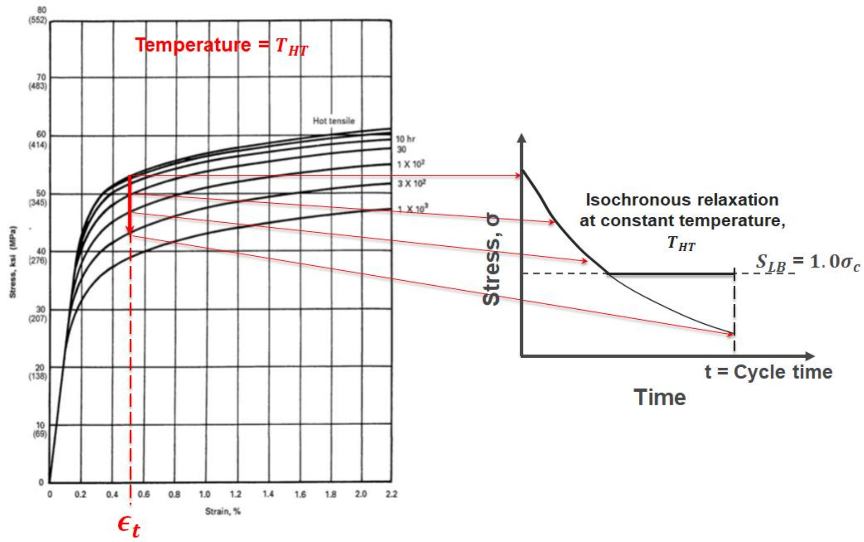

Figure 29: Illustration of determining Stress relaxation profile for creep damage calculation in Method 1.

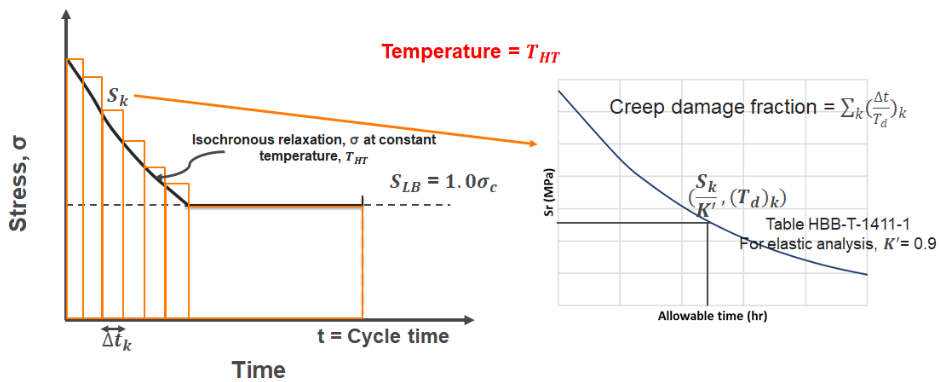

Figure 30: Illustration of calculating creep damage fraction in Method 1.

	At OD on stress classification line-1 shown in Figure 28	***At ID on stress classification line-1 shown in Figure 28***	***At OD on stress classification line-2 shown in Figure 28***	***At ID on stress classification line-2 shown in Figure 28***
	Start-up/shut-down cycle	***Start-up/shut-down cycle***	***Start-up/shut-down cycle***	***Start-up/shut-down cycle***
$\Delta\epsilon_t$	0.0356 %	0.0465 %	0.0387 %	0.0537 %
T_{HT}	770°C	740°C	767.3°C	737.3°C
$S_{LB} = \sigma_c$	22.67	22.67	22.63	22.63
K' (Table HBB-T-1411-1) for elastic analysis	0.9	0.9	0.9	0.9
Creep damage fraction per cycle (from *Table 21*)	5.89e-5	5.91e-5	6.31e-5	6.82e-5
Design cycles, n	30*365=10950	30*365=10950	30*365=10950	30*365=10950
Creep damage fraction, D_c	***0.65***	***0.65***	***0.69***	***0.75***

Table 20: Sample creep damage fraction, D_c calculation according to Method 1.

At OD on stress classification line-1 shown in Figure 28						***At OD on stress classification line-2 shown in Figure 28***					
Time (hr)	S_k ***(MPa)***	$\frac{S_k}{K'}$ ***(MPa)***	$(T_d)_k$ ***(hr)***	Δt_k ***(hr)***	$(\frac{\Delta t}{T_d})_k$	***Time (hr)***	S_k ***(MPa)***	$\frac{S_k}{K'}$ ***(MPa)***	$(T_d)_k$ ***(hr)***	Δt_k ***(hr)***	$(\frac{\Delta t}{T_d})_k$
0	6.11e1	6.79e1	2.04e5	1	4.91e-6	0	6.65e1	7.39e1	1.90e5	1	5.26e-6
1	6.11e1	6.79e1	2.04e5	1	4.91e-6	1	6.65e1	7.39e1	1.90e5	1	5.26e-6
2	6.11e1	6.79e1	2.04e5	1	4.91e-6	2	6.65e1	7.39e1	1.90e5	1	5.26e-6
3	6.11e1	6.79e1	2.04e5	1	4.91e-6	3	6.65e1	7.39e1	1.90e5	1	5.26e-6
4	6.11e1	6.79e1	2.04e5	1	4.91e-6	4	6.65e1	7.39e1	1.90e5	1	5.26e-6
5	6.11e1	6.79e1	2.04e5	1	4.91e-6	5	6.65e1	7.39e1	1.90e5	1	5.26e-6
6	6.11e1	6.79e1	2.04e5	1	4.91e-6	6	6.65e1	7.39e1	1.90e5	1	5.26e-6
7	6.11e1	6.79e1	2.04e5	1	4.91e-6	7	6.65e1	7.39e1	1.90e5	1	5.26e-6
8	6.11e1	6.79e1	2.04e5	1	4.91e-6	8	6.65e1	7.39e1	1.90e5	1	5.26e-6
9	6.11e1	6.79e1	2.04e5	1	4.91e-6	9	6.65e1	7.39e1	1.90e5	1	5.26e-6
10	6.11e1	6.79e1	2.04e5	1	4.91e-6	10	6.65e1	7.39e1	1.90e5	1	5.26e-6
11	6.11e1	6.79e1	2.04e5	1	4.91e-6	11	6.65e1	7.39e1	1.90e5	1	5.26e-6
12	6.11e1	6.79e1	2.04e5			12	6.65e1	7.39e1	1.90e5		
Creep damage fraction per cycle					***5.89e-5***	***Creep damage fraction per cycle***					***6.31e-5***

At ID on stress classification line-1 shown in Figure 28						***At ID on stress classification line-2 shown in Figure 28***					
Time (hr)	S_k ***(MPa)***	$\frac{S_k}{K'}$ ***(MPa)***	$(T_d)_k$ ***(hr)***	Δt_k ***(hr)***	$(\frac{\Delta t}{T_d})_k$	***Time (hr)***	S_k ***(MPa)***	$\frac{S_k}{K'}$ ***(MPa)***	$(T_d)_k$ ***(hr)***	Δt_k ***(hr)***	$(\frac{\Delta t}{T_d})_k$
0	8.11e1	9.01e1	2.03e5	1	4.92e-6	0	9.38e1	1.04e2	1.76e5	1	5.68e-6
1	8.11e1	9.01e1	2.03e5	1	4.92e-6	1	9.38e1	1.04e2	1.76e5	1	5.68e-6
2	8.11e1	9.01e1	2.03e5	1	4.92e-6	2	9.38e1	1.04e2	1.76e5	1	5.68e-6
3	8.11e1	9.01e1	2.03e5	1	4.92e-6	3	9.38e1	1.04e2	1.76e5	1	5.68e-6
4	8.11e1	9.01e1	2.03e5	1	4.92e-6	4	9.38e1	1.04e2	1.76e5	1	5.68e-6
5	8.11e1	9.01e1	2.03e5	1	4.92e-6	5	9.38e1	1.04e2	1.76e5	1	5.68e-6
6	8.11e1	9.01e1	2.03e5	1	4.92e-6	6	9.38e1	1.04e2	1.76e5	1	5.68e-6
7	8.11e1	9.01e1	2.03e5	1	4.92e-6	7	9.38e1	1.04e2	1.76e5	1	5.68e-6
8	8.11e1	9.01e1	2.03e5	1	4.92e-6	8	9.38e1	1.04e2	1.76e5	1	5.68e-6
9	8.11e1	9.01e1	2.03e5	1	4.92e-6	9	9.38e1	1.04e2	1.76e5	1	5.68e-6
10	8.11e1	9.01e1	2.03e5	1	4.92e-6	10	9.38e1	1.04e2	1.76e5	1	5.68e-6
11	8.11e1	9.01e1	2.03e5	1	4.92e-6	11	9.38e1	1.04e2	1.76e5	1	5.68e-6
12	8.11e1	9.01e1	2.03e5			12	9.38e1	1.04e2	1.76e5		
Creep damage fraction per cycle					***5.91e-5***	***Creep damage fraction per cycle***					***6.82e-5***

Table 21: Sample calculation to determine creep damage fraction, D_c per cycle from stress-time history according to Method 1.

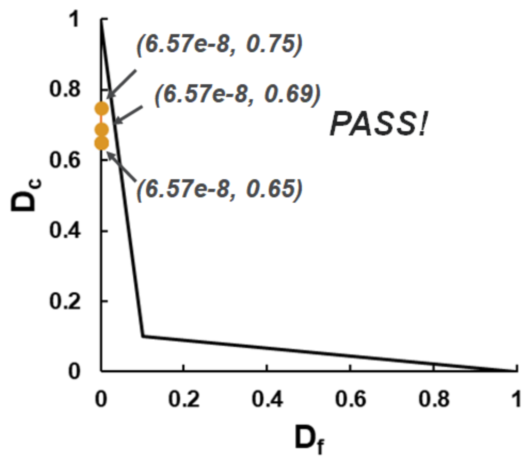

Figure 31: Illustration of creep-fatigue design check. Plotted data are results from analysis according to Method 1.

Step 6: Strain-controlled time-independent buckling check
This design check was not performed as buckling is not expected under these loading conditions.

Design calculations based on Method 2
Steps 1, 2, 3, 4, and 6 in Method 2 are same as in Method 1 and therefore only Step 5 is discussed here.
Step 5: Creep-fatigue damage check
Method 2 is applicable only if the primary plus secondary stress intensity $(P + Q)$ remains less than S_y for all service loading and if peak stresses are minimal.
For a design to be acceptable, the following relation must be satisfied:

$$\sum_j (\frac{n}{N_d})_j + \sum_k (\frac{\Delta t}{T_d})_k \leq D$$

where D is the total creep-fatigue damage and the first and second terms on the left side are fatigue damage, D_f and creep damage, D_c, respectively. In the fatigue damage term, $(n)_j$ is the number of repetitions of cycle type j and $(N_d)_j$ is the number of design allowable cycles for respective cycle type; while in the creep damage term, $(T_d)_k$ is the allowable time duration for a given stress at the maximum temperature occurring in the time interval k and $(\Delta t)_k$ is the duration of the time interval k.
The design allowable cycles for fatigue damage is determined by entering fatigue curves at total strain range, ϵ_t. Total strain range, ϵ_t is calculated using equation HBB-T-1432-16:

$$\Delta\varepsilon = \Delta\epsilon_1 + \Delta\epsilon_2$$

where $\Delta\epsilon_1$ is the maximum equivalent strain range calculated from the elastic analysis of under primary and secondary loading together, according to Section III, Division 5, HBB-T-1413. $\Delta\epsilon_2$ is the creep strain increment per stress cycle. $\Delta\epsilon_2$ can be determined by entering the isochronous stress-strain curves at the O'Donnell-Porowski core stress, σ_c (determined in Method 1, Step 4) and maximum metal temperature for the stress cycle time, including hold times between transient (instead of total service life). Alternatively, $\Delta\epsilon_2$ can be calculated by dividing the creep strain accumulated during the entire service life by the number of stress cycles during the entire service life. We used the latter option.

Creep damage for each service load cycle is evaluated from the von Mises stress profile, determined from elastically calculated stresses, versus time profile for this load cycle. Using the stress-time profile and the hold time temperature, T_{HT} during the cycle, creep damage fraction can be calculated according to the illustration in Figure 32. As mentioned before, we only considered the start-up/shut-down service load cycle and the day time (12 hr) during the cycle for creep damage fraction calculation.

Table 22 and 23 shows few sample calculations of determining creep damage fraction, D_c and fatigue damage fraction, D_f, respectively, according to Method -2. Similar to Method 1, Method 2 also uses creep-fatigue interaction diagram to determine whether a design passes creep-fatigue damage check. Comparing (D_f, D_c) with the damage envelop in creep-fatigue interaction diagram the design is found to be passed according to Method 2.

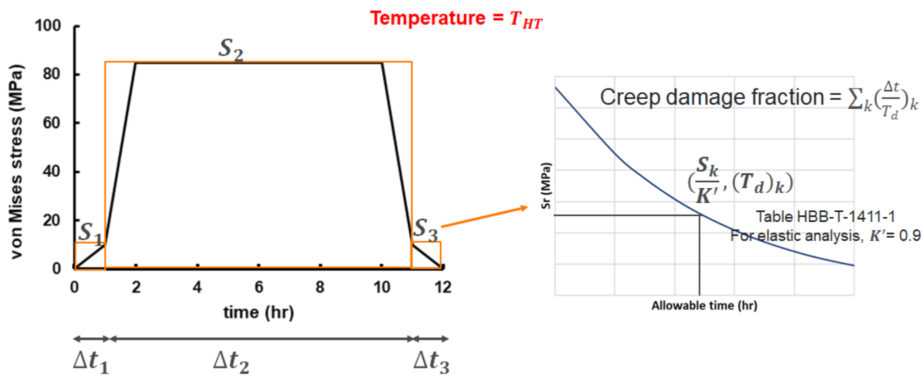

Figure 32: Illustration of calculating creep damage fraction in Method 2.

At OD on stress classification line-1 shown in Figure 28						*At OD on stress classification line-2 shown in Figure 28*					
T_{HT} = 770°C *S_y at T_{HT} = 490 MPa (Method 2 is applicable!)*						*T_{HT} = 767.3°C* *S_y at T_{HT} = 492.3 MPa (Method 2 is applicable!)*					
Time (hr)	***S_k (MPa)***	***$\frac{S_k}{K'(=0.9)}$ (MPa)***	***$(T_d)_k$ (hr)***	***Δt_k (hr)***	***$(\frac{\Delta t}{T_d})_k$***	***Time (hr)***	***S_k (MPa)***	***$\frac{S_k}{K'(=0.9)}$ (MPa)***	***$(T_d)_k$ (hr)***	***Δt_k (hr)***	***$(\frac{\Delta t}{T_d})_k$***
0	0	-	-	-	-	0	0	-	-	-	-
1	7.88	8.76	390230	1	2.56e-6	1	9.05	10.06	385957	1	2.59e-6
2	57.17	63.52	195295	10	5.12e-4	2	59.93	66.59	212754	10	4.70e-5
10	57.17	-	-	-	-	10	59.93	-	-	-	-
11	7.88	8.76	390230	1	2.56e-6	11	9.05	10.06	385957	1	2.59e-6
12	0	-	-	-	-	12	0	-	-	-	-
Creep damage fraction per cycle					*5.63e-5*	*Creep damage fraction per cycle*					*5.21e-5*
Creep damage fraction, D_c					***0.62***	***Creep damage fraction, D_c***					***0.57***
At ID on stress classification line-1 shown in Figure 28						*At ID on stress classification line-2 shown in Figure 28*					
T_{HT} = 740°C *S_y at T_{HT} = 512 MPa (Method 2 is applicable!)*						*T_{HT} = 737.3°C* *S_y at T_{HT} = 513 MPa (Method 2 is applicable!)*					
Time (hr)	***S_k (MPa)***	***$\frac{S_k}{K'(=0.9)}$ (MPa)***	***$(T_d)_k$ (hr)***	***Δt_k (hr)***	***$(\frac{\Delta t}{T_d})_k$***	***Time (hr)***	***S_k (MPa)***	***$\frac{S_k}{K'(=0.9)}$ (MPa)***	***$(T_d)_k$ (hr)***	***Δt_k (hr)***	***$(\frac{\Delta t}{T_d})_k$***
0	0	-	-	-	-	0	0	-	-	-	-
1	9.72	10.8	394482	1	2.53e-6	1	10.55	11.7	395103	1	2.53e-6
2	74.01	82.23	200011	10	4.50e-5	2	86.03	95.59	196367	10	5.09e-5
10	74.01	-	-	-	-	10	86.03	-	-	-	-
11	9.72	10.8	394482	1	2.53e-6	11	10.55	11.7	395103	1	2.53e-6
12	0	-	-	-	-	12	0	-	-	-	-
Creep damage fraction per cycle					*5.51e-5*	*Creep damage fraction per cycle*					*5.60e-5*
Creep damage fraction, D_c					***0.60***	***Creep damage fraction, D_c***					***0.61***

Table 22: Sample calculation to determine creep damage fraction, D_c per cycle from stress-time history according to Method 2.

	At OD on stress classification line-1 shown in Figure 28		***At OD on Stress classification line-2 shown in Figure 28***	
	Start-up/shut-down cycle	***Cloud event***	***Start-up/shut-down cycle***	***Cloud event***
T^{max}	770°C	770°C	767.3°C	767.3°C
$\Delta\epsilon_1$	0.0356 %	0.0360 %	0.0377 %	0.0376 %
$\Delta\epsilon_2$	2.23e-12%	0	6.05e-13%	0
$\Delta\varepsilon$	0.0356 %	0.0360 %	0.0387 %	0.0386 %
Design allowable cycles, N_d	> 1e12	> 1e12	> 1e12	> 1e12
Design cycles, n	30*365=10950	30*365*5=54750	30*365=10950	30*365*5=54750
Fatigue damage fraction, D_f	***6.57e-8***		***6.57e-8***	

Table 23: Sample calculations of determining fatigue damage fraction, D_f according to Method 2.

Design calculations based on Method 3

This method is applicable only if the elastically-calculated stresses remain below the material yield stress, S_y. In the discussion of design calculation based on Method 2, it is shown that the elastically-calculated stress for this sample problem is always less than S_y and therefore Method 3 is applicable.

For primary load design, Method 3 uses the same procedures in Method 1 which is based on elastic analysis. For ratcheting and creep-fatigue design checks, however, this method uses inelastic analysis where material's constitutive response is described by an elastic-creep model. The description of the elastic-creep material model is provided above. Design calculations related to ratcheting and creep-fatigue damage are discussed for Method 3.

Step 1a: Defining service loads and design loads (for primary load design check)

Same as in Method 1 Step 1.

Step 1b: Defining service loads and design loads (for ratcheting and creep-fatigue evaluation)

In this method, separate weather related load cannot be separated from a standard daily load cycle. For this sample problem, therefore, the design load, shown in Figure 21, is considered as the service load.

Step 2a: Transient elastic thermo-mechanical analysis for each service load case (for primary load design check)

Same as in Method 1 Step 2.

Step 2b: Transient elastic-creep thermo-mechanical analysis for each service load case (for ratcheting and creep-fatigue evaluation)

We used MOOSE (Multiphysics Object Oriented Simulation Environment), an open source finite element solver to perform the transient elastic-creep thermo-mechanical analyses under the loading conditions mentioned in Step 1b. The analysis was repeated until a steady state cyclic response was achieved.

Step 3: Primary load design check

Same as in Method 1 Step 3.

Step 4: Ratcheting check

To determine ratcheting strain Method 3 requires to run the analysis using elastic-creep material model, described above, and monitor the maximum effective strain, $\sqrt{\frac{2}{3}\varepsilon:\varepsilon}$ at the beginning and end of the cycle. The criterion is that the ratcheting strain does not exceed 2% at any point of the structure for base metal. Figure 33 plots the maximum effective strain at the critical tube location as a function of cycle count. Extrapolating the maximum effective strain out to design life of the tube, i.e. 30 years (=30*365 cycles), gives the ratcheting strain of 0.00565% which is less than 2%.

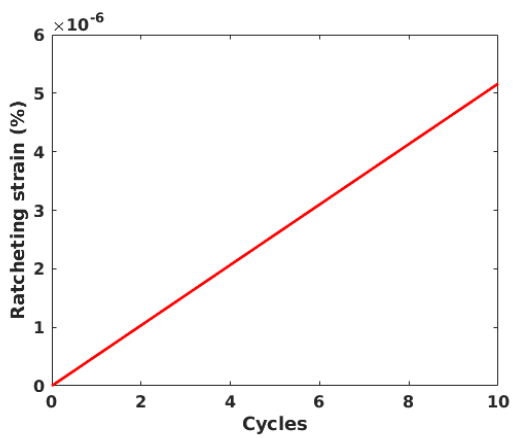

Figure 33 Maximum ratcheting strain in the structure versus number of cycles determined from elastic-creep thermo-mechanical analysis.

Step 5: Creep-fatigue damage check

Once steady cyclic response was achieved in the analysis, the temperature, stress, strain, time history for a single cycle of the periodic loading were extracted. To determine fatigue damage fraction, the effective strain range, $\Delta\varepsilon$ was first computed from the strain history according to Section III, Division 5, HBB-T-1413 with $\nu^* = 0.5$ for inelastic analysis. Fatigue damage fraction, D_f was then calculated from $\Delta\varepsilon$ using rainflow counting and Miner's rule. Figure 34 plots temperature, von Mises stress, and effective strain range profiles at four critical locations of the tube after a steady cyclic response was achieved. Table 24 shows details of the fatigue damage fraction calculation according to Method 3. The von Mises effective stress, $\sigma_{eff}(t)$ was used to determine the creep damage fraction. Figure 35 illustrates the method of creep damage fraction, D_c calculation and Table 25 reports details of the calculation for four critical locations in the structure. All four sets of (D_f, D_c) fall inside the damage envelop in the creep-fatigue interaction diagram which means according to Method 3 the design passes creep-fatigue damage check.

According to Table HBB-1411-1 in Section III, Division 5 of ASME Code, a design margin (i.e, K') is applied to the effective stress while determining the allowable rupture time from the design rupture table. ASME Code recommends to use $K' = 0.9$ for elastic analysis and $K' = 0.67$ for inelastic analysis. However, he creep damage fraction calculation is repeated in Table 26 with $K' = 0.9$. The history behind the ASME stress factors is somewhat murky, but given the lower consequences of failure we recommend a stress factor of 0.9 for all analysis, including inelastic analysis.

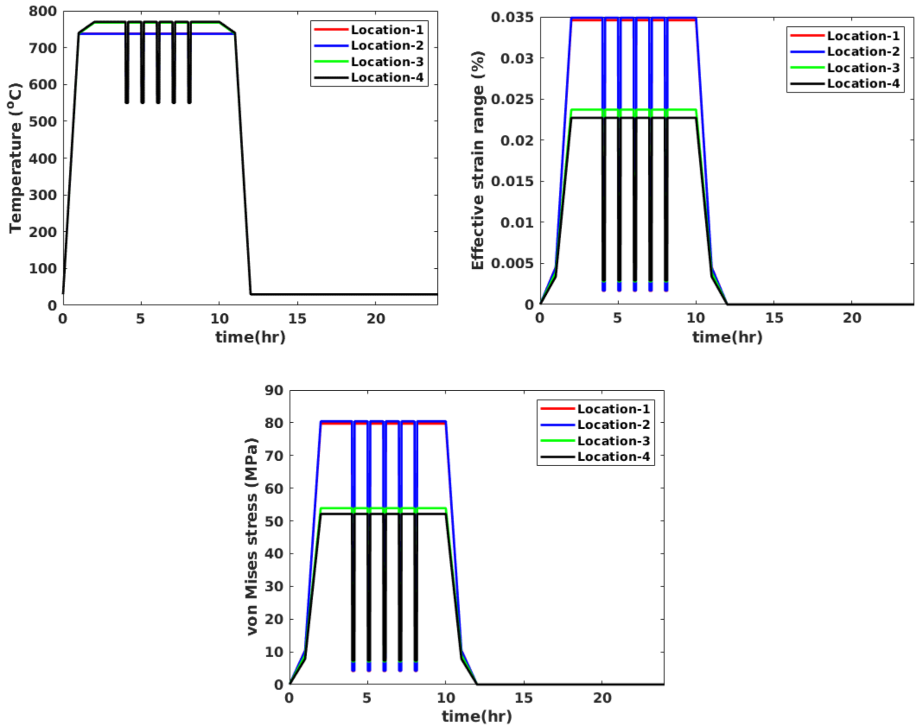

Figure 34 Temperature, effective strain range, and von Mises stress profiles at four critical location of the tube after a steady cyclic response is achieved in the elastic-creep thermo-mechanical analysis.

	Location-1		Location-2		Location-3		Location-4	
T^{max}	738.0°C		737.4°C		768.0°C		770.0°C	
Strain range and corresponding cycle frequency according to rainflow counting of effective strain range, $\Delta\varepsilon$	0.0346%	0.0329%	0.0349%	0.0332%	0.0237%	0.0209%	0.0302%	0.0273%
	1	5	1	5	1	5	1	5
Design allowable cycles, N_d	> 1e12	> 1e12	> 1e12	> 1e12	> 1e12	> 1e12	> 1e12	> 1e12
Fatigue damage fraction per cycle	6.0e-12		6.0e-12		6.0e-12		6.0e-12	
Design cycles, n	30*365=10950		30*365=10950		30*365=10950		30*365=10950	
Fatigue damage fraction, D_f	***6.57e-8***		***6.57e-8***		***6.57e-8***		***6.57e-8***	

Table 24: Sample calculation of determining fatigue damage fraction, D_f according to Method 3.

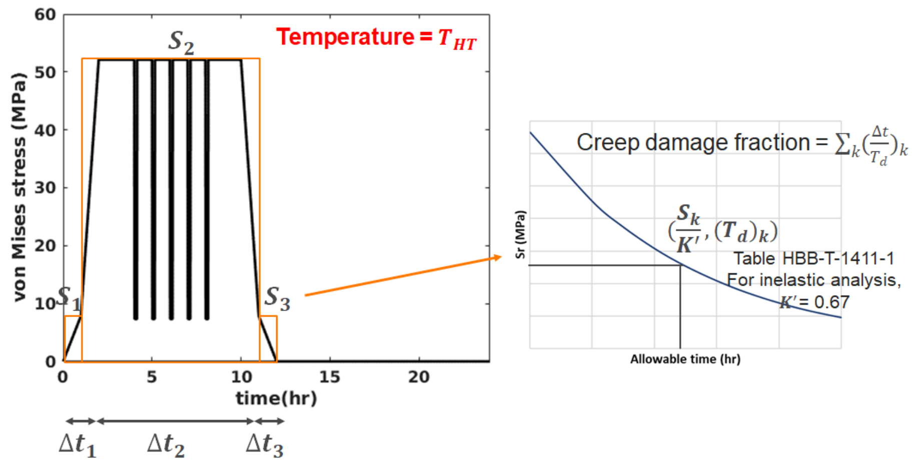

Figure 35: Illustration of calculating creep damage fraction in Method 3.

	Location-1			Location-2			Location-3			Location-4		
Temperature during hold, T_{HT}	738.0°C			737.4°C			768.0°C			770.0°C		
von Mises effective stress, σ_{eff} *(MPa)* and corresponding time	10.5	79.7	10.5	10.4	80.4	10.4	8.9	53.9	8.9	7.8	52.1	7.8
interval, Δt_k *(hr)*	1	10	1	1	10	1	1	10	1	1	10	1
$\frac{S_k (=\sigma_{eff})}{K'(=0.67)}$	15.7	119.0	15.7	15.5	120.0	15.5	13.3	80.4	13.3	11.6	77.8	11.6
Allowable time, $(T_d)_k$ *(hr)*	3.8e5	1.4e5	3.8e5	3.9e5	1.4e5	3.9e5	3.8e5	1.7e5	3.8e5	3.8e5	1.7e5	3.8e5
$(\frac{\Delta t}{T_d})_k$	2.6e-6	7.2e-5	2.6e-6	2.6e-6	7.2e-5	2.6e-6	2.7e-6	5.9e-5	2.7e-6	2.6e-6	5.8e-5	2.6e-6
Creep damage fraction per cycle	7.71e-5			7.75e-5			6.45e-5			6.32e-5		
Design cycles, n	30*365=10950			30*365=10950			30*365=10950			30*365=10950		
Creep damage fraction, D_c	***0.84***			***0.85***			***0.71***			***0.69***		

Table 25: Sample calculation of determining creep damage fraction, D_c according to Method 3.

	Location-1			Location-2			Location-3			Location-4		
Temperature during hold, T_{HT}	738.0°C			737.4°C			768.0°C			770.0°C		
von Mises effective stress, σ_{eff} *(MPa)* and corresponding time	10.5	79.7	10.5	10.4	80.4	10.4	8.9	53.9	8.9	7.8	52.1	7.8
interval, Δt_k *(hr)*	1	10	1	1	10	1	1	10	1	1	10	1
$\frac{S_k (=\sigma_{eff})}{K'(=0.67)}$	11.7	88.6	11.7	11.6	89.3	11.6	9.9	59.9	9.9	8.7	57.9	8.7
Allowable time, $(T_d)_k$ *(hr)*	3.9e5	2.1e5	3.9e5	4.0e5	2.1e5	4.0e5	3.9e5	2.3e5	3.9e5	3.9e5	2.4e5	3.9e5
$(\frac{\Delta t}{T_d})_k$	2.5e-6	4.7e-5	2.5e-6	2.5e-6	4.7e-5	2.6e-6	2.6e-6	4.3e-5	2.6e-6	2.6e-6	4.6e-5	2.6e-6
Creep damage fraction per cycle	5.24e-5			5.24e-5			4.82e-5			4.76e-5		
Design cycles, n	30*365=10950			30*365=10950			30*365=10950			30*365=10950		
Creep damage fraction, D_c	***0.57***			***0.57***			***0.53***			***0.52***		

Table 26: Repeat of calculations in Table 10 by changing $K' = 0.67$ to $K' = 0.9$.

Sample problem 2

For sample problem 2 we considered a tube in an external tubular receiver. The receiver has parabolic reflectors at the back of the tubes which help reduce the variation in the circumferential heat flux distribution on the tube. Figure 36 shows the schematic of the tubular receiver. The tube is 10.5 m long, 42.2 mm diameter, and 1 mm thick. Heat flux on the tube is non uniform both along the length and circumference. We considered only one type of cycle for this problem which represent heat flux on the day of spring equinox. Figure 37 plots the loading profiles of maximum flux incident, salt inlet and outlet temperature, and salt pressure during day (10 hrs). The salt considered for this problem is $MgCl_2$/KCl binary molten salt. The mass flow rate of the salt is 44.5 kg/s. Salt inlet and outlet temperatures are 700°C and 720°C, respectively. The tube can freely expand both in radial and axial direction, however warping is not allowed in the axial direction. Figure 38 shows the heat flux and tube outer wall temperature distribution at noon. The design life of the tube is considered to be 4.4 years. Design calculations according all three methods are provided below without detailed discussion.

This sample problem quickly runs through the design checks for all three methods. See problem 1 for a more detailed walk through of each method.

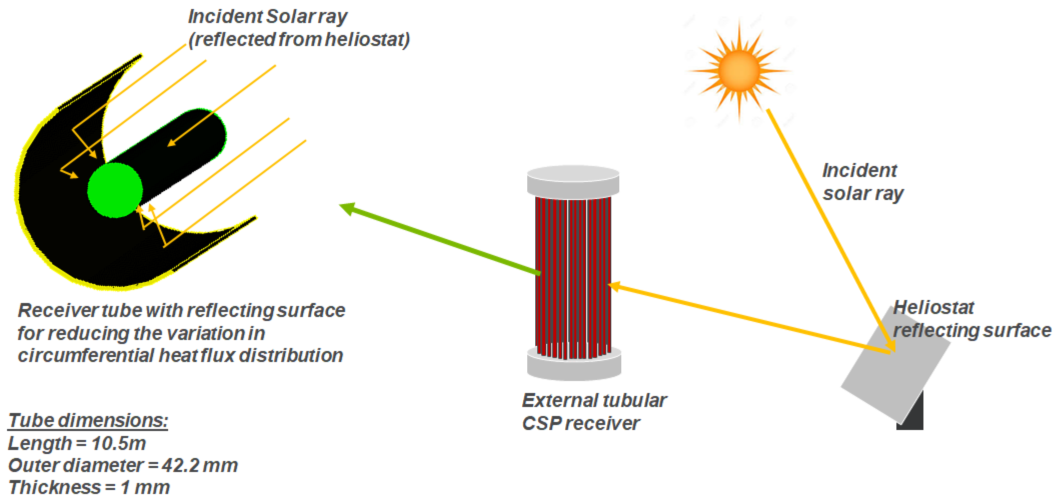

Figure 36: Schematic of an external tubular receiver (Sample problem 2).

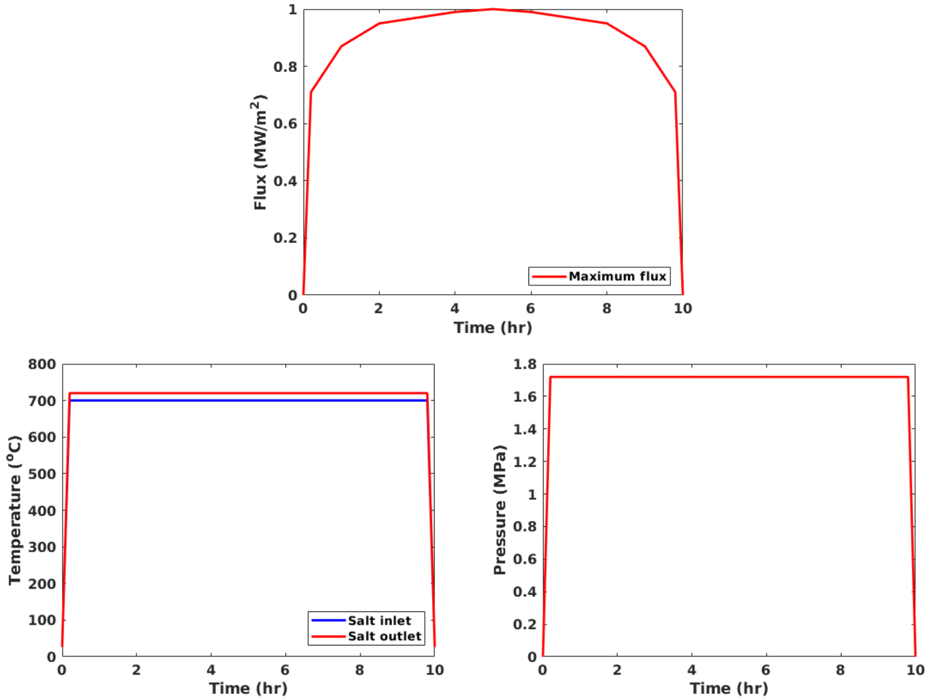

Figure 37: (Sample problem 2) Loading profiles of maximum flux incident, salt inlet and outlet temperature, and salt pressure during day. Only one type of cycle is considered. Receiver operation time per day is 10 hours. Loading profiles shown are only for the tube considered for design study.

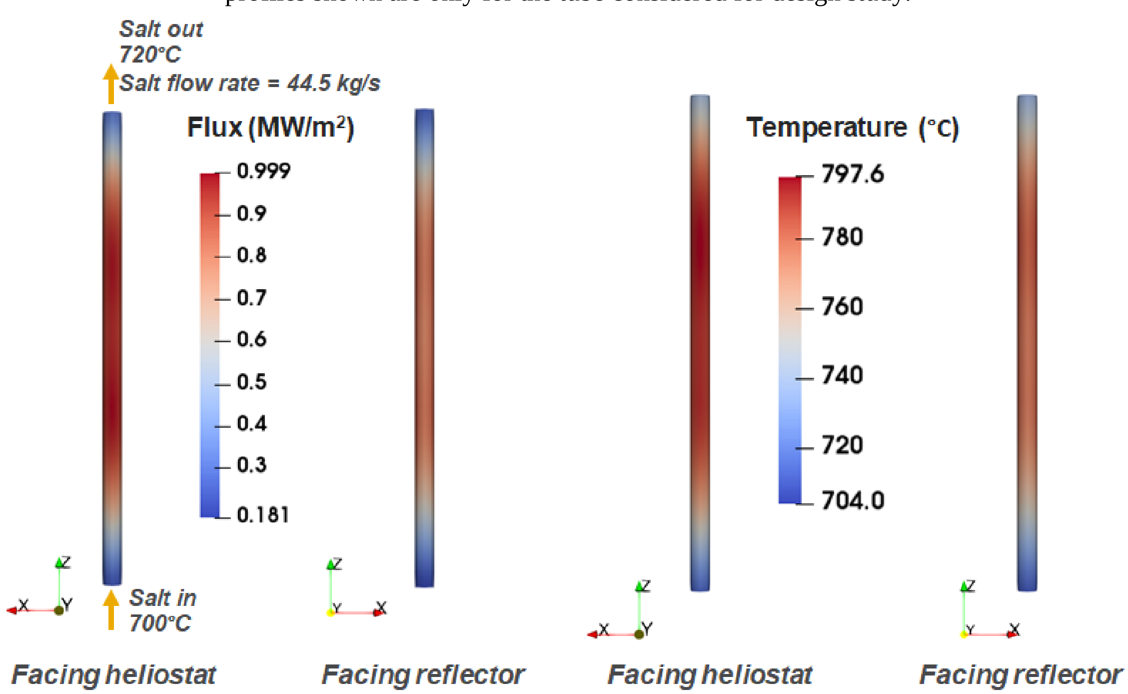

Figure 38: (Sample problem-2) Contour plot of flux incident on tube and tube outer wall temperature at noon.

Design calculations based on Method 1

Step 1: Defining service loads and design loads

As we considered only one type of loading condition, the loading profile shown in Figure 37 can be considered as both the design load and service load.

Step 2: Transient elastic thermo-mechanical analysis for each service load case and stress classification

We used MOOSE (Multiphysics Object Oriented Simulation Environment), an open source finite element solver to perform the transient elastic thermo-mechanical analyses. We classify pressure as primary load and temperature gradient as secondary load. There is no peak load. Figure 39 shows elastic stresses at noon at a critical location of the tube.

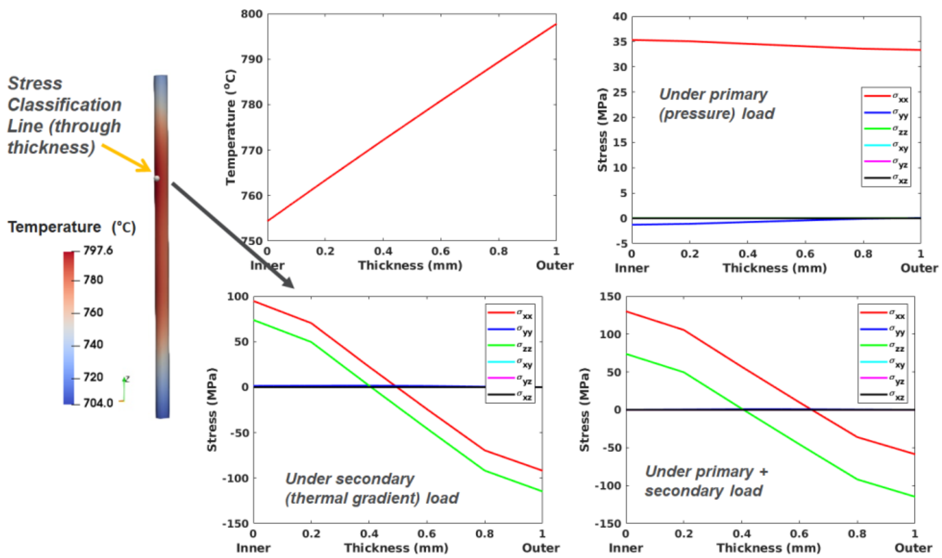

Figure 39: (Sample problem-2) Through thickness temperature and elastic stresses at a critical location of the tube at noon.

Step 3: Primary load design check

See Table 27.

Max. General primary membrane stress intensity, P_m	34.90 MPa
Max. Combined primary membrane plus bending stress intensity, $P_L + P_b$	36.76 MPa
Maximum metal temperature, T_{max}	797.6 °C
Allowable stress, S_o at T_{max}	36.89 MPa
Design criteria -1: $P_m \leq S_o$	***PASS !***
Design criteria -2: $P_L + P_b \leq 1.5\, S_o$	***PASS !***

Table 27: (Sample problem-2) Primary load design checks along the stress classification line shown in Figure 39, according to Method 1,2, &3.

Step 4: Ratcheting check

See Table 28.

	Stress classification line shown in Figure 39
$T_{wall\ averaged}^{max}$	776.4 °C
$T_{wall\ averaged}^{min}$	30 °C
T^{max}	797.6 °C
S_{yH} (at $T_{wall\ averaged}^{max}$)	451.16 MPa
S_{yL} (at $T_{wall\ averaged}^{min}$)	621.0 MPa
$S_y = (S_{yH} + S_{yL})/2$	536.08 MPa
K	1.5
$K_t = (K+1)/2$	1.25
$(P_L + \frac{P_b}{K_t})_{max}$	36.39 MPa
$(Q_R)_{max}$	114.76 MPa
$X = (P_L + \frac{P_b}{K_t})_{max}/S_y$	0.0679
$Y = (Q_R)_{max}/S_y$	0.2147
Z using Section III, Division 5, Figure HBB-T-1332-1	0.0679
σ_c from $Z = \frac{\sigma_c}{S_{yL}}$	42.17
Service life (considering whole day as service time per day)	4.4 years = 38544 hours
Ratcheting strain at the end of service life	0.151%
Ratcheting design criteria: 2% for base metal	***PASS!***

Table 28: (Sample problem-2) Ratcheting design checks according to Method-1&2.

Step 5: Creep-fatigue damage check

See Table 29 for fatigue damage fraction calculation, Tables 30 and 31 for creep damage calculation, and Figure 40 for creep-fatigue damage check.

	At OD on stress classification line shown in Figure 39	***At ID on stress classification line shown in Figure 39***
T^{max}	797.6°C	754.4°C
Hot temperature	797.6°C	754.4°C
Cold temperature	30°C	30°C
Hot time	10hr*(4.4*365) =16060 hr	10hr*(4.4*365) =16060 hr
Cold time	14hr*(30*365) =22484 hr	14hr*(30*365) =22484 hr
S_{rH}	78.4 MPa	126.4 MPa
S_{rL}	Not required	Not required
S_m at T^{max}	218.9 MPa	253.5 MPa
$3\bar{S}_m$	406.8 MPa	506.7 MPa
$\Delta\epsilon_{max}$	0.0583 %	0.0659 %
K	1 (no peak stress)	1 (no peak stress)
$K\Delta\epsilon_{max}$	0.0582 %	0.0659 %
E	169216 MPa	173104 MPa
$3\bar{S}_m/E$	0.240%	0.293%
K_e	1	1
K'_v	1	1
K_v	1	1
$\frac{S^*}{S}$	1	1
$\Delta\epsilon_{mod}$	0.0582 %	0.0659 %
$\Delta\epsilon_c$	0.094e-3%	0
ϵ_t	0.0583 %	0.0659 %
Design allowable cycles, N_d	> 1e12	> 1e12
Design cycles, n	4.4*365=1602	4.4*365=1606
Fatigue damage fraction, D_f	***1.60e-9***	***1.60e-9***

Table 29: (Sample problem-2) Sample calculation of determining fatigue damage fraction, D_f according to Method 1.

	At OD on stress classification line shown in Figure 39	***At ID on stress classification line shown in Figure 39***
$\Delta\epsilon_t$	0.0583 %	0.0659 %
T_{HT}	797.6°C	754.4°C
$S_{LB} = \sigma_c$	42.17 MPa	42.17 MPa
K' (Table HBB-T-1411-1) for elastic analysis	0.9	0.9
Creep damage fraction per cycle (from *Table 31*)	6.16e-4	1.42e-4
Design cycles, n	4.4*365=1602	4.4*365=1602
Creep damage fraction, D_c	***0.99***	***0.28***

Table 30: (Sample problem-2) Sample creep damage fraction, D_c calculation according to Method 1.

At OD on stress classification line shown in Figure 39						*At ID on stress classification line shown in Figure 39*					
Time (hr)	S_k *(MPa)*	$\frac{S_k}{K'}$ *(MPa)*	$(T_d)_k$ *(hr)*	Δt_k *(hr)*	$(\frac{\Delta t}{T_d})_k$	*Time (hr)*	S_k *(MPa)*	$\frac{S_k}{K'}$ *(MPa)*	$(T_d)_k$ *(hr)*	Δt_k *(hr)*	$(\frac{\Delta t}{T_d})_k$
0	9.87E+01	1.10E+02	1.62E+04	1	6.16E-05	0	1.14E+02	1.27E+02	7.04E+04	1	1.42E-05
1	9.87E+01	1.10E+02	1.62E+04	1	6.16E-05	1	1.14E+02	1.27E+02	7.04E+04	1	1.42E-05
2	9.87E+01	1.10E+02	1.62E+04	1	6.16E-05	2	1.14E+02	1.27E+02	7.04E+04	1	1.42E-05
3	9.87E+01	1.10E+02	1.62E+04	1	6.16E-05	3	1.14E+02	1.27E+02	7.04E+04	1	1.42E-05
4	9.87E+01	1.10E+02	1.62E+04	1	6.16E-05	4	1.14E+02	1.27E+02	7.04E+04	1	1.42E-05
5	9.87E+01	1.10E+02	1.62E+04	1	6.16E-05	5	1.14E+02	1.27E+02	7.04E+04	1	1.42E-05
6	9.87E+01	1.10E+02	1.62E+04	1	6.16E-05	6	1.14E+02	1.27E+02	7.04E+04	1	1.42E-05
7	9.87E+01	1.10E+02	1.62E+04	1	6.16E-05	7	1.14E+02	1.27E+02	7.04E+04	1	1.42E-05
8	9.87E+01	1.10E+02	1.62E+04	1	6.16E-05	8	1.14E+02	1.27E+02	7.04E+04	1	1.42E-05
9	9.87E+01	1.10E+02	1.62E+04	1	6.16E-05	9	1.14E+02	1.27E+02	7.04E+04	1	1.42E-05
10	9.87E+01	1.10E+02	1.62E+04			10	1.14E+02	1.27E+02	7.04E+04		
Creep damage fraction per cycle					***6.16e-4***	*Creep damage fraction per cycle*					***1.42e-4***

Table 31: (Sample problem-2) Sample calculation of creep damage fraction, D_c per cycle from stress-time history according to Method 1.

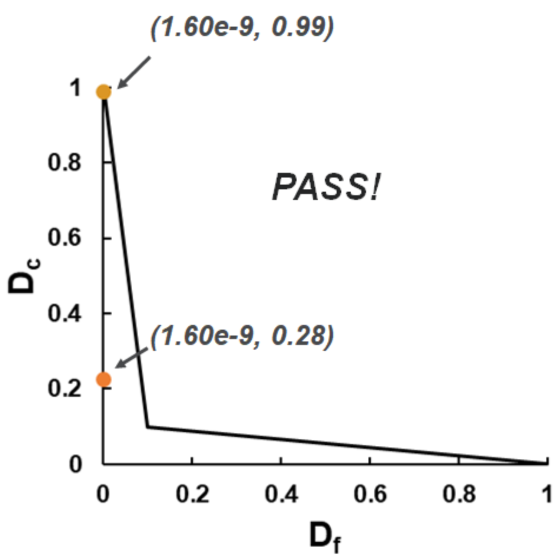

Figure 40: (Sample problem-2) Illustration of creep-fatigue design check. Plotted data are results from analysis according to Method 1.

Step 6: Strain-controlled time-independent buckling check
This design check was not performed as buckling is not expected for this loading condition.

Design calculations based on Method 2
Steps 1, 2, 3, 4, and 6 in Method 2 are same as in Method 1.
Step 5: Creep-fatigue damage check
See Figure 41 and Table 32 for creep damage fraction calculation, Table 33 for fatigue damage calculation, and Figure 42 for creep-fatigue damage check.

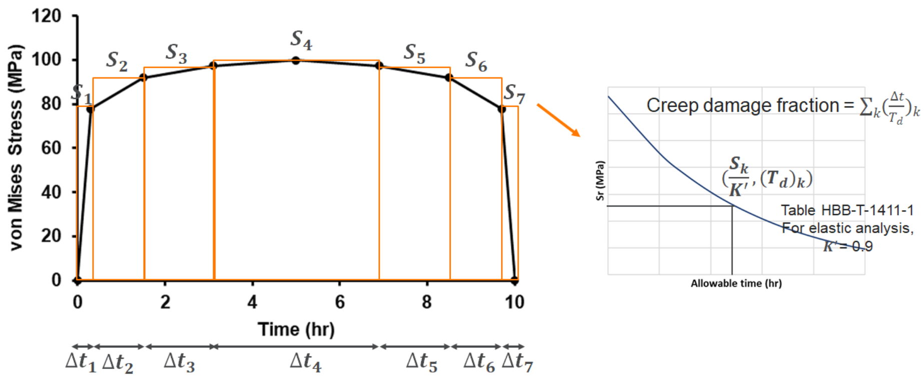

Figure 41: (Sample problem-2) Illustration of calculating creep damage fraction in Method 2.

At OD on stress classification line shown in Figure 39					
T_{HT} = 797.6°C *S_y at T_{HT} = 465.2 MPa (Method 2 is applicable!)*					
Time (hr)	***S_k (MPa)***	***$\frac{S_k}{K'(=0.9)}$ (MPa)***	***$(T_d)_k$ (hr)***	***Δt_k (hr)***	***$(\frac{\Delta t}{T_d})_k$***
0.3	77.84	86.49	67197	0.3	4.46E-06
1.5	91.83	102.03	24022	1.2	5.00E-05
3.1	97.4	108.22	17667	1.6	9.06E-05
5	99.84	110.93	14885	3.8	2.55E-04
6.9	97.4	108.22	17667	1.6	9.06E-05
8.5	91.83	102.03	24022	1.2	5.00E-05
9.7	77.84	86.49	67197	0.3	4.46E-06
10	0	0			
Creep damage fraction per cycle					*5.45e-3*
Creep damage fraction, D_c					***0.87***

Table 32: (Sample problem-2) Sample calculation of creep damage fraction, D_c per cycle from stress-time history according to Method 2.

	At OD on stress classification line shown in Figure 39
T^{max}	797.6°C
$\Delta\epsilon_1$	0.0583 %
$\Delta\epsilon_2$	0.094e-3%
$\Delta\varepsilon$	0.0583 %
Design allowable cycles, N_d	> 1e12
Design cycles, n	4.4*365=1602
Fatigue damage fraction, D_f	***1.60e-9***

Table 33: (Sample problem-2) Sample calculation of fatigue damage fraction, D_f according to Method 2.

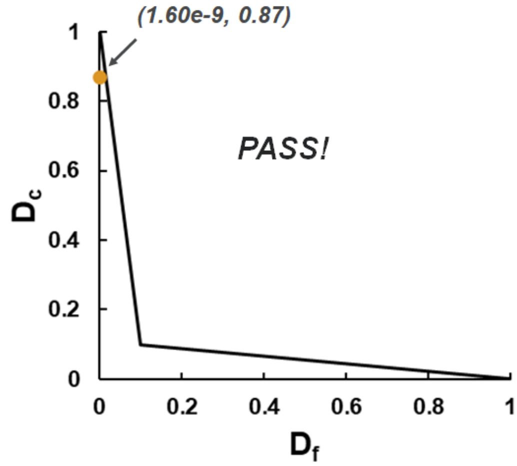

Figure 42: (Sample problem-2) Illustration of creep-fatigue design check. Plotted data are results from analysis according to Method 2.

Design calculations based on Method 3

Step 1: Defining service loads and design loads (for primary load design check)

Same as in Method 1 Step 1.

Step 2a: Transient elastic thermo-mechanical analysis for each service load case (for primary load design check)

Same as in Method 1 Step 2.

Step 2b: Transient elastic-creep thermo-mechanical analysis for each service load case (for ratcheting and creep-fatigue evaluation)

We used MOOSE (Multiphysics Object Oriented Simulation Environment), an open source finite element solver to perform the transient elastic-creep thermo-mechanical analyses under the loading conditions mentioned in Step 1. The analysis was repeated until a steady state cyclic response was achieved.

Step 3: Primary load design check

Same as in Method 1 Step 3.

Step 4: Ratcheting check

See Figure 43.

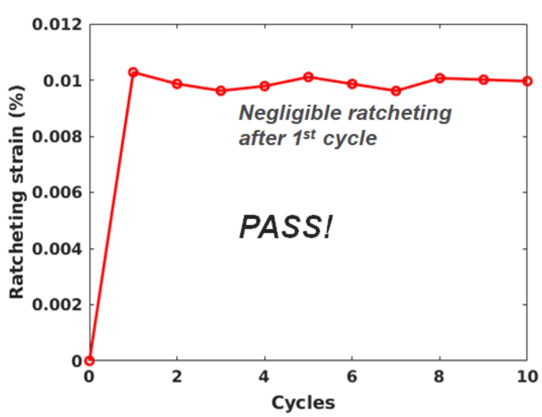

Figure 43: (Sample problem-2) Maximum ratcheting strain in the structure versus number of cycles determined from elastic-creep thermo-mechanical analysis.

Step 5: Creep-fatigue damage check

Once steady cyclic response was achieved in the analysis, the temperature, stress, and strain-time history for a single cycle of the periodic loading were extracted. Figure 44 plots the temperature, and the steady cyclic effective strain range and von Mises effective stress at the critical location of the tube. Details of the fatigue damage fraction calculation is provided in Table 20. The tube experiences negligible fatigue damage.

Figure 45 illustrates creep damage fraction evaluation from the steady cyclic von Mises effective stress profile. Detail calculation of creep damage fraction is provided in Table 21. Using a stress factor of 0.67 the creep damage fraction at the critical location of the tube is found to be more than 1, which means the design of the tube does not pass the creep-fatigue damage check according to Method 3.However, as discussed in sample problem 1 a factor of 0.67 is too conservative for CSP systems. Therefore, the creep damage fraction calculation is repeated in Table 22 with $K' = 0.9$. This gives much lower creep damage fraction and the design passes the creep-fatigue damage check.

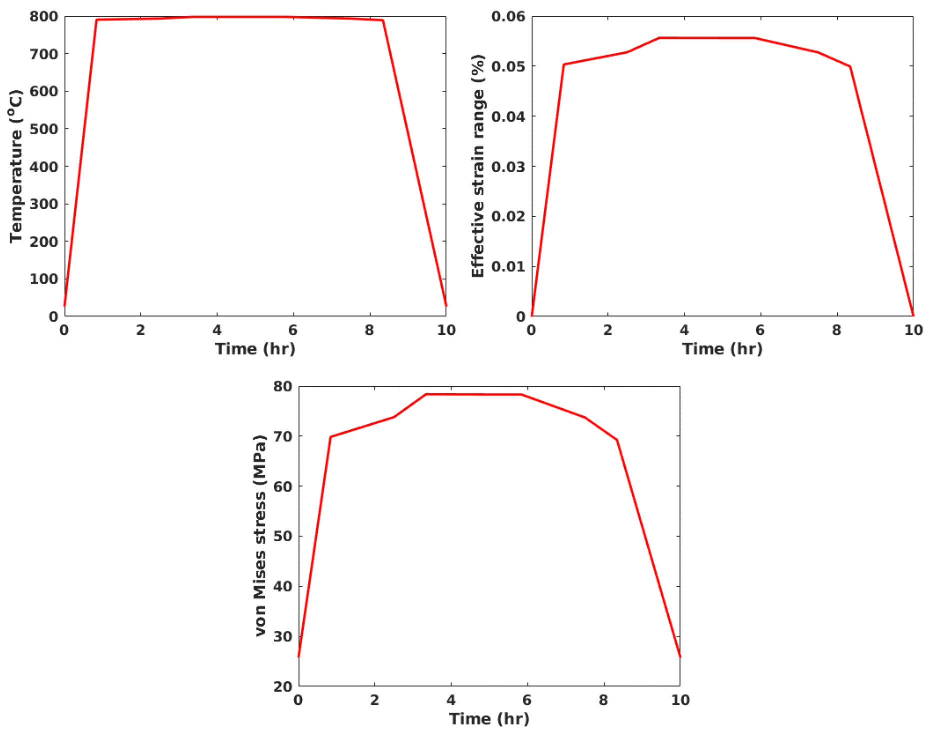

Figure 44: (Sample problem-2) Temperature, effective strain range, and von Mises stress profiles at the critical location of the tube after a steady cyclic response is achieved in the elastic-creep thermo-mechanical analysis.

	At the critical location
T^{max}	797.6°C
Strain range and corresponding cycle frequency according to rainflow counting of effective strain range, $\Delta\varepsilon$	0.0557%
	1
Design allowable cycles, N_d	> 1e12
Design cycles, n	4.4*365=1606
Fatigue damage fraction, D_f	***1.602e-9***

Table 34: (Sample problem-2) Sample calculation of fatigue damage fraction, D_f according to Method 3.

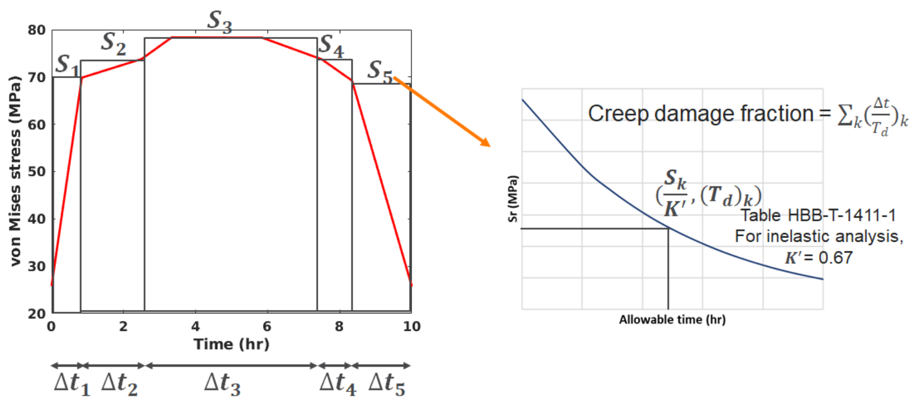

Figure 45: (Sample problem-2) Illustration of calculating creep damage fraction in Method 3.

	At the critical location				
Temperature during hold, T_{HT}	797.6°C				
von Mises effective stress, σ_{eff} *(MPa)* and corresponding time interval, Δt_k *(hr)*	69.8	73.8	78.3	73.7	69.2
	0.84	1.66	5	0.84	1.66
$\frac{S_k\ (=\sigma_{eff})}{K'(=0.67)}$	104.2	110.1	116.9	110.0	103.3
Allowable time, $(T_d)_k$ *(hr)*	21794	15737	9691	15839	22718
$(\frac{\Delta t}{T_d})_k$	3.85E-05	1.05E-04	5.16E-04	5.30E-05	7.31E-05
Creep damage fraction per cycle	7.86e-4				
Design cycles, n	4.4*365=1606				
Creep damage fraction, D_c	***1.26 (FAIL!)*** ***D_c is more than 1.***				

Table 35: (Sample problem-2) Sample calculation of creep damage fraction, D_c according to Method 3.

	At the critical location				
Temperature during hold, T_{HT}	797.6°C				
von Mises effective stress, σ_{eff} *(MPa)* and corresponding time interval, Δt_k *(hr)*	69.8	73.8	78.3	73.7	69.2
	0.84	1.66	5	0.84	1.66
$\frac{S_k\ (=\sigma_{eff})}{K'(=0.9)}$	77.6	82.0	87.0	81.9	76.9
Allowable time, $(T_d)_k$ *(hr)*	101224	84383	65244	84765	103904
$(\frac{\Delta t}{T_d})_k$	8.30E-06	1.97E-05	7.66E-05	9.91E-06	1.60E-05
Creep damage fraction per cycle	1.30e-4				
Design cycles, n	4.4*365=1606				
Creep damage fraction, D_c	***0.21 (PASS!)*** ***(D_f, D_c) falls inside the damage envelop in the creep-fatigue interaction diagram***				

Table 36: (Sample problem-2) Repeat of calculations in Table 21 by changing $K' = 0.67$ to $K' = 0.9$.

Comparison of the design methods

In general, Method 1 requires the most designer effort, followed by Method 2, and Method 3. So generally designers will prefer 2 and 3, depending on if they want to use elastic analysis (2) or are comfortable with a simple inelastic analysis (3).

All methods predict fatigue damage in the two sample components is negligible. However, the relative conservative of the three approaches can be assessed by comparing the creep damage fractions for each method for the two sample problems. Table 37 provides this comparison, using a stress factor of 0.9 for Method 3.

	Method 1	Method 2	Method 3
Sample Problem 1	0.75	0.61	0.57
Sample Problem 2	0.99	0.87	0.21

Table 37: Creep damage fraction for each problem and for each design method

Methods 1 and 2 produce comparable creep damage fractions, which makes sense as they are fundamentally both the ASME design by elastic analysis method, with simplifications for Method 1. Full inelastic analysis, at least with a stress factor of 0.9, produces much less over conservative results. With a factor of 0.67 the results of inelastic analysis are comparable to the damage fractions predicted by the elastic analysis methods.

Summary

These sample problems, along with the current design allowables, will be distributed to the project design expert and three CSP system vendors for evaluation. This will fulfill our project Q6 deliverable. We will request they use sample problem 1 (the simple linear gradient tube) as the reference problem for the round robin, but will provide sample problem 2 as well, as it is a more realistic geometry.

Our final milestone is the complete, finalized design method. We are on track to provide this at the start of Q7 (November 2019). For the design data only the creep-fatigue diagram is not final. This diagram will be finalized when the remaining INL creep-fatigue tests are completed.

The design methods presented here will be recommended in the final report. The only remaining item to address, which will be completed in Q7, is a method for assessing buckling in receiver structures. As long as the receiver design provides axial strain relief, the thermomechanical loading is unlikely to cause buckling. However, the combination of the thermomechanical loading plus an external wind load does have the potential to buckle a receiver tube. ANL has developed a buckling method based on the isochronous curves developed in this project. The Q7 report will detail this method and provide example calculations. The method will also be provided in our final report.

Additional work will focus on interpreting the INL sheet tests to provide modified design constants for very thin structures and on finalizing the design methods and preparing the final, detailed design method report.

Task 3

Force controlled testing

Task 3 will examine the effect of different material forms on the design models (particularly fatigue). Specifically, we will be looking at Alloy 740H sheet in this task. Due to the nature of sheet fatigue testing, it is not feasible to do fully reversed, strain controlled testing, as the material would buckle during the compression. Furthermore, it is more difficult to measure strain directly from the sheet specimens without causing deformation from the pressure imposed by the extensometers onto the specimen. As a result, the sheet metal testing will be performed in load control, with an R=0.1 (minimum stress will be 10% of maximum stress). To allow for a more direct comparison of tests, several force controlled, R=0.1 tests were performed on plate material. The results of the three tests run this quarter are shown below in Figure 46. Loads were chosen based on strain controlled test results. Initially the force was chosen to match the peak stress achieved during the 1% delta strain tests. This resulted in too short of a fatigue life, so a force was chosen to match the near-steady state stress after the initial peak. Additional tests at 750°C will be performed in the next quarter. A machine and grips have been identified for sheet testing, and these tests will also begin shortly.

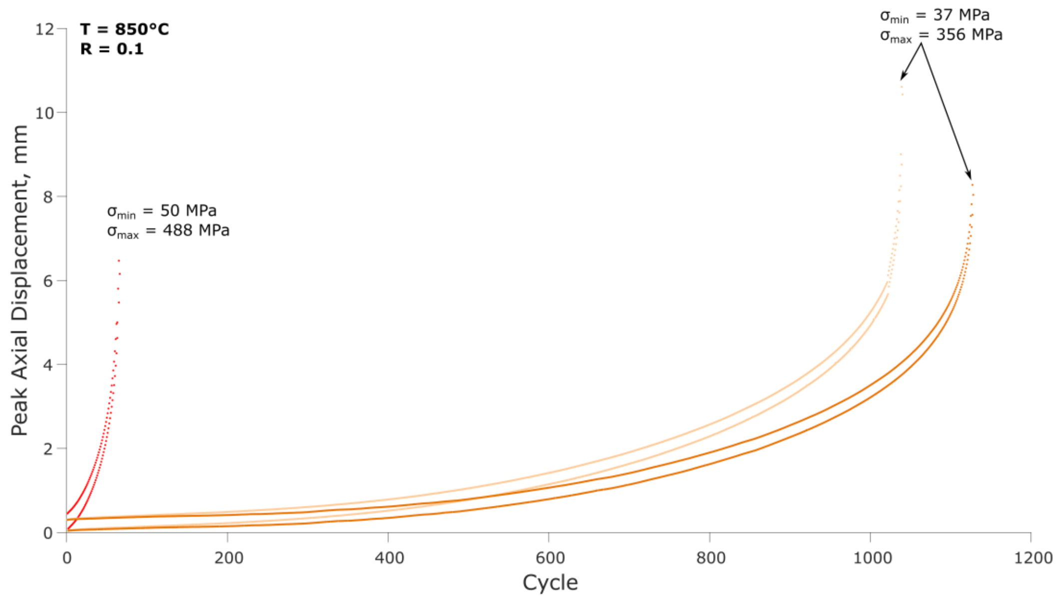

Figure 46. Displacement vs cycle of load controlled tests.

Summary

Testing performed on the plate material will provide a basis for expectation of the sheet metal testing. These tests will also be included in the Argonne design models moving forward. A summary of the load controlled, Alloy 740H plate tests is shown in Table 38.

Temp.	Hold time	R	σ_{min}	σ_{max}	At Cycle 10		Midlife			Machine Cycles to Failure
					axial $disp_{max}$	axial $disp_{min}$	cycle used	axial $disp_{max}$	axial $disp_{min}$	
(^{o}C)	(min)		MPa	MPa	mm	mm		mm	mm	
850	0	0.1	50	488	0.642	0.256	33	1.496	1.082	66
850	0	0.1	37	356	0.327	0.064	500	1.050	0.780	1040
850	0	0.1	37	356	0.314	0.053	550	0.920	0.652	1128

Table 38. Results of load controlled, Alloy 740H plate material tested during Q6.

References

[1] Special Metals, http://www.specialmetals.com/assets/smc/documents/alloys/inconel/inconel-alloy-740-h.pdf.
[2] American Society of Mechanical Engineers Boiler & Pressure Vessel Code Case 2702, 2011.
[3] Purgert, R. et al. *Boiler materials for ultra supercritical coal power plants*. DOE technical report, 2015.
[4] Jena, P. S. M., et al. "Low cycle fatigue behavior of nickel base superalloy IN 740H at 760° C: Influence of fireside corrosion atmosphere." *International Journal of Fatigue* 116: pp. 623-633, 2018.

[5] Zhang, S. and Takahashi, Y. "Evaluation of high temperature strength of a Ni-based Alloy 740H for advanced ultra-supercritical power plant." In *Advances in Materials Technology for Fossil Power Plants: Proceedings from the Seventh International Conference*, Waikoloa, Hawaii, USA, 2014.
[6] Kocks, U. "Realistic constitutive relations for metal plasticity." Materials Science and Engineering A 317:, pp. 181-187, 2001.
[7] Mecking, H., Nicklas, B., Zarubova, N., et al. "A 'universal' temperature scale for plastic flow." Acta Metallurgica 34(3): pp. 527-535, 1986.
[8] Zhang, Shengde, and Yukio Takahashi. "Creep and Creep-Fatigue Deformation and Life Assessment of Ni-Based Alloy 740H and Alloy 617." In *ASME 2018 Pressure Vessels and Piping Conference*, pp. V06AT06A060-V06AT06A060. American Society of Mechanical Engineers, 2018.